BIOPROTA

**Key Issues in Biosphere Aspects of Assessment of the Long-term Impact of Contaminant Releases Associated with Radioactive Waste Management**

*THEME 2: Task 4:*

# Model Intercomparison with Focus on Accumulation in Soil

Main Contributors: A Albrecht (Task Leader), C Damois, E Kerrigan, R Klos, G Smith, M Thorne, M Willans and H Yoshida

**JUNE 2005**

TABLE OF CONTENTS

FOREWORD VI

1. THE INTERCOMPARISON 1
   1.1 Objectives of the Assessment Model Comparison Task 1
   1.2 Contamination pathways and parameterisation 1
   1.3 Participating organisations and codes 5
2. RESULTS OF THE WELL SCENARIO 16
   2.1 Evolution with time 16
   2.2 Radionuclide concentration in the soil at 10000 years 24
3. DISCUSSION 26
   3.1 Radionuclide concentration in the soil compartment 26
   3.2 Human dose 30
4. RESULTS OF THE RIVER SCENARIOS 35
   4.1 Concept and approaches for the river scenario 35
   4.2 Results 35
   4.3 Discussion 37
5. SUMMARY AND CONCLUSIONS 39
6. REFERENCES 40

Appendices

1. APPENDIX A: ANALYTICAL SOLUTION OF THE EQUATION GOVERNING THE RADIONUCLIDE ACTIVITY IN THE SOIL: APPROXIMATE EXPRESSION
2. APPENDIX B: RADIONUCLIDES CONCENTRATION WITH THE CONDITION OF INCREASED IRRIGATION RATE IN EDF MODELLING FACTOR OF 2.66
3. APPENDIX C: RADIONUCLIDES CONCENTRATION IN THE SOIL, SATURATED ROCK AND UNSATURATED IN UKAEA MODELLING

## LIST OF FIGURES

Figure 1: Concept of the well and the river water contamination scenarios..... 2

Figure 2: Processes considered in the BNFL soil model ..... 7

Figure 3: Nirex model for well scenario ..... 11

Figure 4: UKAEA model used for the well scenario ..... 13

Figure 5: Cl-36 concentration in the soil [Bq/m$^3$] as a function of time as modelled by the different participants (log-log scale) ..... 17

Figure 6: Cl-36 concentration in the soil [Bq/m$^3$] as a function of time as modelled by the different participants (linear scale) ..... 17

Figure 7: Se-79 concentration in the soil [Bq/m$^3$] as a function of time as modelled by the different participants (log-log scale) ..... 18

Figure 8: Se-79 concentration in the soil (Bq/m$^3$) as a function of time as modelled by the different participants (double linear scale) ..... 19

Figure 9: Tc-99 concentration in the soil [Bq/m$^3$] as a function of time as modelled by the different participants (log-log scale) ..... 20

Figure 10: Tc-99 concentration in the soil [Bq/m$^3$] as a function of time as modelled by EDF (linear scale) ..... 20

Figure 11: I-129 concentration in the soil [Bq/m$^3$] as a function of time as modelled by the different participants (log-log scale) ..... 21

Figure 12: I-129 concentration in the soil [Bq/m$^3$] as a function of time as modelled by the different participants (linear scale) ..... 22

Figure 13: Np-237 concentration in the soil [Bq/m$^3$] as a function of time as modelled by the different participants (linear scale) ..... 22

Figure 14: Ra-226 concentration in the soil [Bq/m$^3$] as a function of time as modelled by the different participants (log-log scale) ..... 23

Figure 15: Pb-210 and Po-210 concentration in the soil [Bq/m$^3$] as a function of time as modelled by the different participants (log-log scale) ..... 24

Figure 16: Radionuclides concentration in the soil after 10,000 years of accumulation ..... 25

Figure 17: Percolation loss rates as a function of soil Kd modelled using equation 1 (i.e. BNFL) and equation 2 (NUMO, ANDRA and others) ..... 28

Figure 18: Irrigation-rate corrected soil concentration of EDF for Se-79 [Bq/m$^3$] compared with results obtained by other participants (log-log scale) ..... 29

Figure 19: Total human doses at 10,000 years ..... 31

Figure 20: Modelled total dose rate for different radionuclides as a consequences of accumulation in the soil for a period of 10,000 years, normalised to the soil radionuclide activity ..... 32

Figure 21: Contribution of exposure pathways to the total dose at 10,000 years (Cl-36, Se-79, Tc-99 and I-129) ..... 34

Figure 22: Contribution of exposure pathways to the total dose at 10,000 years (Np-237, Ra-226, Pb-210 and Po-210) ..... 34

Figure 23 : Schematic representation of flooding river water contaminating agricultural soil .....35

Figure 24: Radionuclide concentration in the soil for river scenario [Bq/m$^3$] as a function of time as modelled by the different participants (log-log scale) .....36

Figure 25: Comparison of concentration in the soil between well scenario and river scenario .....38

Figure 26: Radionuclide concentration in the soil with the increased irrigation rate of EDF (Cl-36).....44

Figure 27: Radionuclide concentration in the soil with the increased irrigation rate of Ed (Se-79).....44

Figure 28: Radionuclide concentration in the soil with the increased irrigation rate of EDF (Tc-99) .....45

Figure 29 Radionuclide concentration in the soil with the increased irrigation rate of EDF (I-129) .....45

Figure 30: Radionuclide concentration in the soil with the increased irrigation rate of EDF (Np-237) .....46

Figure 31 Radionuclide concentration in the soil with the increased irrigation rate of EDF (Ra-226) .....46

Figure 32: Radionuclide concentration in the soil in UKAEA modelling.....47

Figure 33: Radionuclide concentration in the unsaturated rock in UKAEA modelling .....47

Figure 34: Radionuclide concentration in the saturated rock in UKAEA modelling .....48

## LIST OF TABLES

Table 1: Scenario dependent parameters and associated values..... 3

Table 2: Nuclide independent parameters and associated values ..... 3

Table 3: Radionuclide dependent parameters and associated values..... 4

Table 4: Relevant information of participating organisations..... 5

Table 5: Irrigation rates applied by EDF..... 8

Table 6: Inhalation related parameters defined by EPRI..... 9

Table 7: Radionuclide dependent parameters for Po-210 used by EPRI.....10

Table 8 : Hydrological parameters used by Nirex for the well scenario.....11

Table 9: Compartment properties in the UKAEA calculation .....14

Table 10: Hydrological parameters as used in the UKAEA calculations.....14

Table 11: Radionuclide dependent parameters of Po-210 as used in the UKAEA calculations .....15

Table 12: Radionuclides concentration in soil the at 10,000 years (Bq/$m^3$) .....25

Table 13: Summary of loss rates calculated by BNFL and NUMO modelling for well scenario .....26

Table 14: Summary of exposure pathways modelled .....30

Table 15: Total human doses at 10,000 years [Sv/y] .....31

Table 16: Radionuclide concentration in the soil at 10,000 years river scenario [Bq/$m^3$]...37

Table 17: Summary of loss rates calculated by BNFL and NUNO modelling for river scenario .....37

# FOREWORD

Assessing the impacts of releases of radioactivity into the environment rely on a great variety of factors. Important among these is an effectively justified level of understanding of radionuclide behaviour in the environment, the associated migration pathways and the processes that contribute to radionuclide accumulation and dispersion among and within specific environmental media. In addition, evaluating the consequences of any radionuclide releases on human health rely on the use of appropriate physiological and dosimetric models for calculating doses and risks. Assessment methods have been developed over several decades based on knowledge of the ecosystems involved, as well as monitoring of previous radionuclide releases to the environment, laboratory experiments and other research.

It is recognised that in some cases data for these assessments are sparse. Particular difficulties arise in the case of long-lived radionuclides, because of the difficulty of setting up relatively long-term monitoring and experimental programmes, and because the biosphere systems themselves will change over the relevant periods, due to natural processes and the potential for interference by mankind.

It is also the case that much radio-ecological research has tended to focus on relatively few radionuclides, eg. Sr-90 and Cs-137. While this research has been relevant to operational effluent discharges and accidental releases, other radionuclides tend to dominate long term impacts as may arise from the migration of radionuclides from solid radioactive waste repositories. Examples include C-14, Cl-36, Se-79, Tc-99, Np-237. The viability of geological disposal concepts and the long-term sustainability of radioactive effluent discharges, together with the safe and effective management of contaminated land and surface stores for solid radioactive wastes can only be considered in the light of a good understanding of the environmental behaviour of such longer lived radionuclides. However, the number of radionuclides involved is relatively small, and the number of important processes associated with migration and accumulation in the biosphere, and the related radiation exposure of humans and other biota, is also relatively limited.

The International Atomic Energy Agency's BIOMASS Theme 1 has provided a basis for identifying, justifying and describing biosphere systems for the purpose of radiological assessment. The development of conceptual and mathematical models has been set out and a protocol developed for the application of data to these models. However the BIOMASS Project did not address the details of uncertainties arising from weaknesses in the information base.

**BIOPROTA Concept**

BIOPROTA provides a forum to address uncertainties in the assessment of the radiological impact of releases of long-lived radionuclides into the biosphere. The programme of work carried out under the auspices of BIOPROTA focuses on these key radionuclides and the various biosphere migration and accumulation mechanisms relevant to those radionuclides. It is understood that there are radio-ecological and other data and information issues which are common to specific assessments required in many countries. The mutual support within a commonly focused project is intended to make more efficient use of skills and resources, and support a transparent and traceable basis for the choices of parameter values as well as for the wider interpretation of information used in the assessments.

The BIOPROTA Project up to December 2004 has been managed and supported financially by:

| Organisation | Representative | Role of organisation | Website |
|---|---|---|---|
| Agence Nationale pour la Gestion des Déchets Radioactifs (ANDRA) | Elisabeth Leclerc-Cessac | ANDRA is responsible for the management of radioactive waste in France. | www.andra.fr |
| Empresa Nacional de Residuos Radiactivos, S.A. (ENRESA) | Julio Astudilio | ENRESA is responsible for the management of radioactive wastes generated in Spain and the decommissioning of nuclear power plants. | www.enresa.es |
| Nexia Solutions Ltd (formerly BNFL Research & Technology) | Mark Willans | Nexia Solutions is a UK BNFL subsiduary company providing technology solutions and services across the nuclear fuel cycle. | www.nexiasolutions.com |
| United Kingdom Nirex Limited (Nirex) | Paul Degnan | Nirex is the radioactive waste management agency with responsibility to develop and advise on safe, environmentally sound and publicly acceptable options for the long-term management of radioactive materials in the UK. | www.nirex.co.uk |
| Nuclear Waste Management Organization of Japan (NUMO) | Shigeru Okuyama | NUMO is the implementing body for the final disposal of vitrified high-level waste packaged from the spent fuel reprocessing plant. It is a government approved organization responsible for identification of a disposal site, and for the construction, operation and maintenance of the repository, closure of the facility, and post-closure institutional control. | www.numo.or.jp |
| Posiva Oy | Ari Ikonen | Posiva is responsible for the management of disposal of spent fuel produced in power reactors in Finland, including siting, licencing, construction and operation of the repository. | www.posiva.fi |
| Svensk Kärnbränslehantering AB (SKB) | Ulrik Kautsky | SKB is responsible for management of Swedish radioactive waste, planning of waste repositories, waste logistics and site selection, including safety analysis, research and development of methods. | www.skb.se |

Since January 2005, the Project has been additionally managed and supported financially by:

| Organisation | Representative | Role of organisation | Website |
|---|---|---|---|
| Electricité de France (EDF) | Carine Damois | EDF is been the main producer of electricity in France. The Laboratoire National Hydraulique et Environnement (LNHE) department works on migration of pollutants in the ground, waste management, water quality, soil contamination, ecotoxicology, ecology, microbiology, health risk assessment, but also fluvial and maritime hydraulics, resource management, industrial | www.edf.fr |

| | | | |
|---|---|---|---|
| | | flows and combustion, meteorology and air quality. | |
| Korea Atomic Energy Research Institute (KAERI) | Yong-Soo Hwang | Kaeri is developing the Korean reference concept for permanent disposal of high-level radioactive waste including spent nuclear fuel and assessing the long term post-closure safety and repository performance. | www.kaeri.re.kr |
| National Cooperative for the Disposal of Radioactive waste (Nagra) | Frits van Dorp | Nagra has more than 30 years experience in the development of disposal concepts for all categories of radioactive waste. Over the years, Nagra has built up extensive technical know-how and has applied this in site characterisation and performance assessment of deep geological repositories. | www.nagra.ch |
| Nuclear Research Institute Rez (NRI) | Ales Laciok | In the Czech Republic, NRI is the research, development and engineering organisation responsible for the development of nuclear power technologies, utilization of radionuclides and radiation in industry and medicine, and with a role to undertake fundamental research to support the long-term management and disposal of radioactive wastes. | www.nri.cz |

The BIOPROTA output is made available for use of others, but the participants and supporting organisations take no responsibility for the use of the material.

**General Objectives**

Overall the intention is to make available the best sources of information to justify modelling assumptions. Particular emphasis is placed on key data required for the assessment of long-lived radionuclide migration and accumulation in the biosphere, and the associated radiological impact, following discharge to the environment or release from solid waste disposal facilities.

The project is driven by assessment needs identified from previous and on-going assessment projects. Where common needs are identified within different assessment projects in different countries, a common effort can be applied to finding solutions. Such solutions may readily take account of the BIOMASS Theme 1 Data Protocol, among other things.

The modelling assumptions considered include the treatment of various features, events and processes (FEPs) of the systems under investigation, the mathematical representation of those FEPs and the choice of parameter values to adopt within those mathematical representations.

The work programme has been organised in three themes:

Theme 1: Development of a Specialised Data-Base for Key Radionuclides and Process Data

Theme 2: Modelling Testing and Development Tasks

Theme 3: Site Characterisation, Experiments and Monitoring.

A full list of all the reports that have been produced under each theme is available from the BIOPROTA website (www.bioprota.com).

**Objectives of the Accumulation in Soil Modelling Task**

The objective of Task 4 within the Theme 2 was to investigate the long term accumulation of radionuclides in soil given a continuous source term.

This Task 4 report includes model descriptions provided by participants and the specification and results of model test calculations designed to investigate the significance of the different model assumptions.

This report has been prepared within the BIOPROTA work programme. The supporting organisations have agreed that BIOPROTA reports will be printed by those organisations in their normal report series. In this case ANDRA is supporting the printing of this Task report, to make it available for a wide audience. ANDRA supports the work of BIOPROTA, but does not necessarily endorse the output. Any question concerning this report should be directed towards the contributors. The report can be obtained directly from ANDRA; it is also available in pdf form at www.bioprota.com along with the other BIOPROTA reports.

**Recommended Citation**

BIOPROTA (2005). Model Intercomparison with focus on accumulation in soil. A report prepared within the international collaborative project BIOPROTA: Key Issues in Biosphere Aspects of Assessment of the Long-term Impact of Contaminant Releases Associated with Radioactive Waste Management. Main Contributors: A Albrecht, C Damois, E Kerrigan, R Klos, G Smith, M Thorne, M Willans and H Yoshida. Published on behalf of the BIOPROTA Steering Committee by ANDRA (Agence nationale pour la gestion des déchets radioactifs), Châtenay-Malabry, France.

# 1. THE INTERCOMPARISON

## 1.1 Objectives of the Assessment Model Comparison Task

In this report, we discuss objectives, definitions and results of an assessment model intercomparison. Focus is given to the long-term accumulation of long lived radionuclides in soils because in many performance assessments the dose rates to human beings largely depend on the radionuclide concentrations in the soil. Two often used scenarios were adapted as means of contamination, the well scenario where contaminated well water is used for irrigation of agricultural land, and a river scenario where contaminated river water floods the agricultural land.

To highlight the impact of the mathematical equations, a review on soil accumulation and leaching is included based on earlier work [Klos, 2000]. To simplify the comparison of model results, all common site- or radionuclide-specific parameters were defined.

The main tasks of the exercise were to test the significance of alternative treatments, and to identify weaknesses in data required to deal sufficiently with the relevant processes. As the last assessment intercomparison exercise was 8 years ago (BIOMOVS, carried out in 1996 and published in 1999; [Klos et al, 1999]) a new comparison of the employed models became justified. The intercomparison also allowed users to check those functionalities of their codes, which have seen new versions in recent years. The possibility for users to test their handling of the code including input, element- and site-specific parameterisation, calculation and output specification should not be seen as trivial, particularly in cases where users participated for the first time in an international intercomparison exercise.

## 1.2 Contamination pathways and parameterisation

### 1.2.1 Scenario description

As the goal of this task is to investigate the radiological impact of different soil contamination scenarios, focus will be given to accumulation in the soil compartment. Two different geosphere biosphere interface zones (GBIZ) are considered in this intercomparison exercise. They are:

- A well scenario, where contamination comes from water extracted from a well. This well water is used for irrigation; and,
- A river scenario, where river water is contaminated by discharging groundwater. The river floods and contaminated water thus reaches the soil compartment.

To help building a common understanding among the participants, a possible conceptual model for the assessment was indicated (Figure 1). Compartments are shown as rectangular boxes, with arrows showing the pathways of the contamination. Solid and dotted lines in the lower part of the figure correspond to the well and river scenarios, respectively.

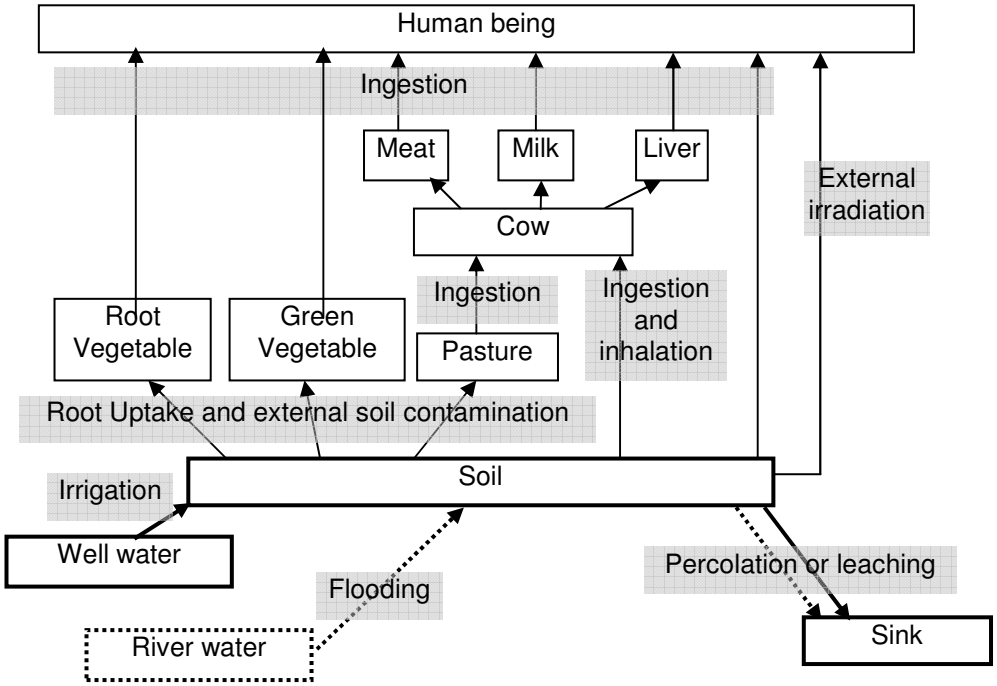


**Figure 1: Concept of the well and the river water contamination scenarios**

For simplicity, the well water (or river water) was assumed to have a constant concentration of 1Bq/L throughout the entire period of the contamination. The soil contamination is calculated for a period of accumulation of up to 10,000 years in both scenarios to check the equilibrium conditions.

The concentrations of the soil compartment are then transcribed to dose values on the basis of a simplified exposure pathway and a pre-described critical group. Accumulation processes and exposure pathways within the food chain have been specified in Figure 1. The considered food chain is relatively simple, considering root and leafy vegetables and grass initially and then cow meat, liver and milk following consumption of fodder by livestock. Direct exposure on contaminated land is also considered. Note that pathways that are dealt with in other BIOPROTA tasks, such as plant contamination via spray irrigation (Theme 2 Task 1) or soil resuspension and inhalation (Theme 2 Task 2) are not considered here. Pathways that have no link to the soil compartment, as is the case for drinking water, have also been neglected. The following radionuclides, defined as priority radionuclides by participants and their institutions, have been considered in the calculations: Cl-36, Se-79, Tc-99, I-129, Np-237, Ra-226 (including Pb-210 and Po-210 as daughter radionuclides, but not appearing at the source).

### 1.2.2 Suggested values for site-specific parameters

Two lists of proposed site-specific parameters and associated values are given in Table 1 and Table 2. They are extracted from the BIOMASS Example Reference Biospheres EBR 2A and 2B, the first describing a well scenario, the second an inundation scenario [IAEA, 2003]. The low flooding rate of the river scenario reflects the low frequency of such events.

**Table 1: Scenario dependent parameters and associated values**

| Parameter | Value | Unit | Source |
|---|---|---|---|
| Well water scenario | | | |
| - Irrigation rate | 2.0E-01 | [m/y] | [1] |
| - Percolation rate | 1.0E-01 | [m/y] | [1] |
| River water scenario | | | |
| - Flooding rate | 5.5E-04 | [m/y] | 1% of the percolation rate |
| - Percolation rate | 5.5E-02 | [m/y] | [1] (Arable area adjacent to river) |

**Table 2: Radionuclide independent parameters and associated values**

| Parameter | Value | Unit | Source |
|---|---|---|---|
| Soil porosity | 5.0E-01 | [-] | [1] |
| Cultivated soil thickness | 3.0E-01 | [m] | [1] |
| Soil grain density | 2.65E+03 | [kg/m$^3$] | [1] |
| Wet soil density | 1.625E+03 | [kg/m$^3$] | [1] |
| Water density | 1.0E+03 | [kg/m$^3$] | [1] |
| Soil-plant transfer factor | | [kg(dw soil)/ kg(fw crop) ] | |
| - green vegetable | 2.0E-04 | | [1],[2] |
| - root vegetable | 2.0E-04 | | [1],[2] |
| - pasture | 2.0E-03 | | [2] |
| Crop annual yield | | [kg(fw)/(m$^2$y)] | |
| - green vegetable | 3.0E+00 | | [1],[2] |
| - root vegetable | 3.0E+00 | | [1],[2] |
| - pasture | 5.0E+00 | | [2] |
| External fraction retained after food processing | | - | |
| - green vegetable | 1.0E+00 | | [2] |
| - root vegetable | 1.0E+00 | | [2] |
| Fodder consumption rate of cow | 7.0E+01 | kg(fw)/d | [1] |
| Soil consumption rate of cow | 6.0E-01 | [kg(wet soil)/d] | [1] |
| Breathing rate of cow | 5.4E+00 | [m$^3$/h] | [1] |
| Occupancy time of cow | 2.4E+01 | [h/d] | [1] |
| Dust level for cow | 5.0E-06 | [kg/m$^3$] | [1] |
| Human consumption rate | | [kg(fw)/y] | |
| - green vegetable | 2.9E+02 | | [1] |
| - root vegetable | 3.2E+02 | | [1] |
| - meat | 2.1E+02 | | [1] |
| - milk | 7.4E+02 | | [1] |
| - liver | 2.0E+01 | | |
| - soil | 8.3E-03 | | [1] |
| Occupancy time of human | 2.92E+03 | [h/y] | [1] |

References of Table 1 and Table 2

[1] IAEA, 2003 "Example Reference Biosphere 2A".

[2] IAEA, 2003 "Example Reference Biosphere 2B".

When individual model approaches diverged from the mathematical models produced by BIOMASS [IAEA, 2003], the user had the freedom to specify parameter values independently.

### 1.2.3 Suggested values for radionuclide-specific parameters

Radionuclide-specific parameters were also suggested by the task leaders. They are shown in Table 3 for all radionuclides occurring at the source including the progeny of Ra-226. This parameter list has been extracted from BIOMASS ERB2A and B with modifications based on the current ANDRA database [ANDRA, 2003] and recent review undertaken by Mike Thorne and Associates for BNFL [Thorne, 2003a].

**Table 3: Radionuclide dependent parameters and associated values**

| Parameter [Unit] | Value [reference] | | | | | | |
|---|---|---|---|---|---|---|---|
| | Cl-36 | Se-79 | Tc-99 | I-129 | Np-237 | Ra-226 | Pb-210 |
| Decay constant [1/y] | 2.3E-06 | 1.1E-05 | 3.3E-06 | 4.4E-08 | 3.2E-07 | 4.3E-04 | 3.1E-02 |
| Ingestion dose coefficient [Sv/Bq] | 9.3E-10 | 2.9E-09 | 6.4E-10 | 1.1E-07 | 1.1E-07 | 2.8E-07 | 1.9E-06 |
| External dose factor [(Sv/h)/(Bq/m$^3$)] | 4.7E-17 | 2.9E-19 | 2.4E-18 | 1.8E-16 | 2.0E-14 | 2.0E-13 | 1.4E-16 |
| Sorption coefficient for soil [m$^3$/kg(dw)] | 5.8E-03 [3] | 7.4E-01 [3] | 1.0E-04 [4] | 5.0E-03 [4] | 3.0E-02 [2],[4] | 5.0E+00 [4] | 5.4E-01 [3] |
| Sorption coefficient for suspended matter [m$^3$/kg(dw)] | 1.0E-01 [3] | 3.0E+00 [3] | 1.0E-02 [4] | 1.0E-02 [3] | 5.0E-01 [4] | 5.0E-01 [4] | 1.0E+01 [3] |
| Plant concentration factor [Bq/kg(fw))/(Bq/kg(dw))] | | | | | | | |
| - green vegetable | 3.0E+02 [4] | 5.0E-02 [3] | 1.0E+01 [1],[2],[4] | 3.0E-02 [4] | 3.0E-03 [4] | 3.0E-03 [4] | 1.0E-03 [3],[4] |
| - root vegetable | 3.0E+02 [4] | 5.0E-02 [3] | 1.0E+01 [1],[2],[4] | 3.0E-02 [4] | 3.0E-03 [4] | 3.0E-03 [4] | 1.0E-03 [4] |
| - pasture | 3.0E+02 [4] | 5.0E-02 [3] | 1.0E+01 [1],[2],[4] | 3.0E-02 [4] | 3.0E-03 [4] | 3.0E-03 [4] | 1.0E-03 [4] |
| Transfer factor to cow product from ingestion | | | | | | | |
| - meat [d/kg(fw)] | 4.1E-02 [3] | 5.4E-01 [3] | 7.5E-04 [4] | 4.0E-03 [4] | 1.0E-04 [1],[2],[4] | 4.0E-04 [4] | 1.0E-02 [4] |
| - milk [d/L] | 1.7E-02 [3] | 3.6E-03 [3] | 7.5E-04 [4] | 1.0E-02 [4] | 5.0E-06 [4] | 4.0E-04 [4] | 1.0E-02 [4] |
| - liver [d/kg(fw)] | 2.0E-02 [4] | 1.0E+01 [5] | 7.5E-04 [4] | 4.0E-03 [4] | 1.0E-02 [4] | 1.0E-02 [4] | 5.0E-01 [4] |

References of Table 3

[1] IAEA, 2003 "Example Reference Biosphere 2A".

[2] IAEA, 2003 "Example Reference Biosphere 2B".

[3] ANDRA, 2003.

[4] Thorne, 2003a.

[5] JNC, 2000.

## 1.3 Participating organisations and codes

### 1.3.1 Organisations

BNFL, UKAEA, EPRI, NUMO, EDF, Nirex, ANDRA and Aleksandria Sciences participated in the intercomparison exercises (Table 4). All organizations contributed to the well scenario calculations; ANDRA, BNFL and NUMO to results for the river scenario.

**Table 4: Relevant information of participating organisations**

| Organisation | Country | Code |
|---|---|---|
| Aleksandria Sciences | Great Britain | TAME |
| ANDRA | France | AQUABIOS |
| BNFL | Great Britain | BIOS |
| EDF | France | OURSON |
| EPRI | USA | AMBER |
| Nirex | Great Britain | Nirex GPA assessment spreadsheet |
| NUMO | Japan | AMBER |
| UKAEA | Great Britain | AMBER |

### 1.3.2 Models and parameters

The general mathematical expression used in many assessment models of the activity of radionuclide *N* in the soil compartment [IAEA, 2003] is:

$$\frac{dN}{dt} = S(t) - \lambda_N N - \lambda_{CH} N - \lambda_I N$$

where,

| | |
|---|---|
| $N$ | is the activity of radionuclide *N* in the soil compartment, [Bq] |
| $S(t)$ | is an external source term of radionuclide *N* to the soil compartment, [Bq/y] |
| $\lambda_N$ | is the decay constant for radionuclide *N*, [1/y] |
| $\lambda_{CH}$ | is the loss rate for radionuclide *N* related to cropping, [1/y] |
| $\lambda_I$ | is the loss rate for radionuclide *N* related to percolation/leaching, [1/y] |

Each participant adapted their model (in most cases developed for their assessment purposes) according to the information given in §1.2.2 and §1.2.3. In the following section, some relevant information on each participant's modelling approach is summarised.

***Aleksandria Sciences***

Aleksandria Sciences (AlekSci) uses TAME [Klos et al., 1996], a code developed for the NAGRA performance assessments. The soil compartment is subdivided into two layers, the top and subsoil. Capillary rise and bioturbation were modelled assuming the same Kd in both layers. Essentially, this means that the soil layers are effectively one and the total inventory is spread out over a larger volume. For dose assessments, root crops, green vegetables, meat and milk have been considered.

***ANDRA***

ANDRA uses AQUABIOS a code with the ability for the implementation of mathematical equations and the handling of very large databases. Technical information, validation and qualification issues and application examples of the current version 7.2 are presented elsewhere [Albrecht and Bonafos 2004]. AQUABIOS uses three independent templates for the definition of (1) mathematical equations (models), (2) element-specific and (3) site-specific parameters. All templates are available for any extension manipulation and parameterization, while maintaining the integrity of the core programme. For each project, a model can be chosen from a list of available models (i.e. multi-element models for radionuclides or toxic chemical substances to calculate dose rates in Sv/y or [mg/(kg day)], respectively, or element specific models such as those developed for Tritium, C-14 or Cl-36). Attached to each model is a choice for element-specific and site-specific parameter databases. Within the template for model definition, dynamic compartments (soils or sediments that are likely to accumulate contaminants with time) and descendant calculations (daughters and granddaughters of radionuclides) can be defined by implementation of analytical solutions of the differential equations. Calculations (both deterministic and stochastic) are carried out step-wise allowing all parameters to be changed as a function of time. Intermediate results are managed by flexible intrinsic functions. The code is multi-localized, allowing the programme to run in different languages (currently French and English). A multitude of import and export functions allows direct exchange with external databases and reporting tools. Multilevel user permissions permit total access to all templates (power users). These can be distinguished from other users with restricted privileges.

In the model transcribed in AQUABIOS, ANDRA describes the soil with a one-component representation. Accumulation is calculated using a box model approach considering irrigation or flooding as the radionuclide input vector and calculating losses on the basis of the overall hydraulic balance and the Kd of the radionuclide of interest.

Note that for Cl-36, ANDRA uses a special model based on the specific activity [Sheppard, 2001] but calculations given here are based on the previous compartment approach.

***BNFL***

BNFL models both cropping and percolation losses (

Figure 2) in BIOS [Willans, 2003].

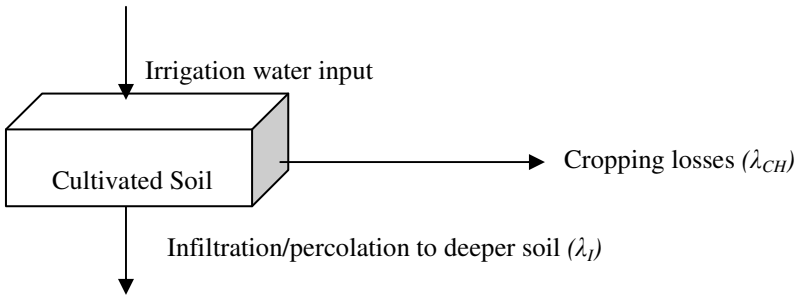


**Figure 2: Processes considered in the BNFL soil model**

The mathematical expression used by BNFL to evaluate the loss terms $\lambda_I$ from the soil compartment is comparable to those used by other participants. It is given here for reference.

$$\lambda_I = \frac{I}{d\theta\left(1+\frac{(1-\theta)\rho_G K_d}{\theta}\right)}$$

where:

| | |
|---|---|
| $I$ | is the infiltration/percolation rate [m/y], |
| $d$ | is the depth of the soil column [m], |
| $\theta$ | is the porosity of the compartment [-], |
| $\rho_G$ | is the particle grain density [kg/m$^3$] and |
| $K_d$ | is the sorption coefficient in the soil [m$^3$/kg]. |

Cropping losses ($\lambda_{CH}$ : mass harvested per unit area and per unit time) were not specified, but considered by BNFL.

$$\lambda_{CH} = I_{CH} T_P / (\rho_G d(1-\theta))$$

where:

$I_{CH}$ is the mass of crop harvested per unit area per unit time [kg/m$^2$/y)],

$\rho_G$ is the particle grain density [kg/m$^3$],

$d$ is the depth of the soil column [m],

$\theta$ is the soil porosity [-]

and $T_P$ is the radionuclide plant transfer factor determined by:

$$T_P = \left(\sum_{plant\ types} plant / soil\ concentration\ ratio\right) / \left(number\ of\ plant\ types\right)$$

Mass of crop harvested per unit area per unit time was set to be 3 kg/m2/y for all plant types. In their exposure modelling, BNFL reconsidered the value of the following two parameters.

- Dry soil consumption rate of cows: 190 kg/y

- Dry soil consumption rate of human: 3.65E-02 kg/y

***EDF***

EDF modelled seasonal change in their calculations [Ciffroy et al.]. Specific daily irrigation rates (Table 5) results in annual irrigation smaller than the value specified for the intercomparison (0.2 m/y). The annual irrigation rate averaged over all plants applied by EDF can be derived by averaging the annual irrigation rate used for the four different plants: (0.084*3+0.050)/4 = 0.075 m/y. This is a factor of 0.38 times smaller than the specified annual irrigation rate. For the dose assessment, EDF considered the ingestion of vegetables, milk, meat and drinking water.

**Table 5: Irrigation rates applied by EDF**

| Plants | Irrigation rate [m/day] | Irrigation term | Remarks |
|---|---|---|---|
| Fruit, root vegetable and leaf vegetable | 5.47E-04 | April, May, June, July and August | Equivalent to 0.084m/y |
| Grass | 5.47E-04 | June, July and August | Equivalent to 0.050 m/y |

***EPRI***

The model used for EPRI:

- considers cropping loss from the soil compartment;
- is based on a complex equation to evaluate transfer to animal products via a combination of inhalation and ingestion; and
- considers Po-210.

The modelling of cropping loses is based on the following equation.

$$\lambda_{CH} = \frac{\sum_{plqnt\,types}\left[\left(CF_{cropi} + S_{cropi}\right)Y_{cropi}\right]}{number\,of\;\;plant\,type} \cdot \frac{1}{(1-\theta_t)\rho}$$

where:

$CF_{crop\ i}$ is the concentration factor for crop 'i' [(Bq/kg(fw) / (Bq/kg(dw))],
$S_{crop\ i}$ is the soil contamination on crop 'i' [kg (dw)/kg(fw)],
$Y_{crop\ i}$ is the crop annual yield of crop 'i' [kg (fw)/m$^2$/y],
$\theta_t$ is the total soil porosity [-], and
$\rho$ is the grain density of soil [kg/m$^3$].

The transfer to animal products via a combination of ingestion and inhalation is based on the following equation:

$$C_{prod} = \underbrace{TF_{proding}\left(C_{fodd}ING_{fodd} + \frac{C_s\;\;ING_{sa}}{(1-\theta_t)\rho + \theta\rho_w}\right)}_{\text{ingestion}} + \underbrace{(BR_a O_{an} C_{airs})TF_{prodinh}}_{\text{inhalation}}$$

where:

$TF_{proding}$ is the transfer factor for ingestion for the animal product, [d/kg(fw)],
$C_{fodd}$ is the radionuclide concentration in the animal fodder, [Bq/kg(fw)],
$TF_{prodinh}$ is the transfer factor for inhalation for the animal product, [d/kg(fw)],
$INGf_{odd}$ is the consumption rate of fodder by the animal, [kg(fw)/d],
$ING_{sa}$ is the consumption rate of soil from the cultivated soil compartment by the animal, [kg(fw)/d],
$\rho_w$ is the density of water, [kg/m$^3$],
$BR_a$ is the breathing rate of the animal, [m$^3$/h],
$O_{an}$ is the occupancy time of the animal in the cultivated soil compartment, [h/d]
$C_{airs}$ is the radionuclide concentration in the air above the cultivated soil compartment, [Bq/m$^3$].

The term $TF_{prodinh}$ is evaluated using the following equation:

$$TF_{prodinh} = TF_{proding} \frac{f_L + f_C f_1(inh)}{f_1(ing)}$$

where:

$f_L$ is the fraction of inhaled activity reaching the systemic circulation of man following transfer across the lung lining [-],
$f_C$ is the fraction of inhaled activity that is cleared to the gastrointestinal tract of man [-],
$f_{1(inh)}$ is the fraction of inhaled activity, cleared to the gastrointestinal tract, that is transferred to the systemic circulation of man [-], and
$f_{1(ing)}$ is the fraction of ingested activity reaching the body fluids in man [-].

Model specific parameters are given in

Table 6.

**Table 6: Inhalation related parameters defined by EPRI**

| Radiouclide | $f_{1(ing)}$ [2] | $f_{1(inh)}$ [2] | $f_C$ [3] | $f_L$ [3] |
|---|---|---|---|---|
| Cl-36 | 1.0E+00 | 1.0E+00 | 5.5E-01 | 1.5E-01 |
| Se-79 | 8.0E-01 | 1.0E-01 | 1.6E-01 | 5.0E-01 |
| Tc-99 | 5.0E-01 | 1.0E-01 | 5.5E-01 | 1.5E-01 |
| I-129 | 1.0E+00 | 1.0E+00 | 1.6E-01 | 5.0E-01 |
| Np-237 | 5.0E-04 | 5.0E-04 | 5.5E-01 | 1.5E-01 |
| Ra-226 | 2.0E-01 | 1.0E-01 | 5.5E-01 | 1.5E-01 |
| Pb-210 | 2.0E-01 | 1.0E-01 | 5.5E-01 | 1.5E-01 |

Nuclide dependent parameters for Po-210 are given in

Table 7.

**Table 7: Radionuclide dependent parameters for Po-210 used by EPRI**

| Parameter | Value | Unit | Source |
|---|---|---|---|
| Decay constant | 1.83E+00 | [1/y] | [1] |
| Ingestion dose coefficient | 1.2E-06 | [Sv/Bq] | [1] |
| External dose factor | 1.05E-18 | [(Sv/h)/(Bq/m$^3$)] | [1] |
| Sorption coefficient for soil | 1.5E-01 | [m$^3$/kg] | [1] |
| Plant concentration factor | | [(Bq/kg)/(Bq/kg)] | [1] |
| - root veg | 2.0E-04 | | |
| - green veg | 2.0E-04 | | |
| - pasture | 2.0E-04 | | |
| Transfer factor to cow products from ingestion [1] | | | |
| - meat | 1.0E-02 | [d/kg] | |
| - milk | 1.0E-02 | [d/L] | |
| - liver | 5.0E-01 | [d/kg] | |
| Translocation factor [1] | | | |
| - root veg | 2.2E-01 | | |
| - green veg | 2.2E-01 | | |
| - pasture | 0.0E+00 | | |
| $f1_{ing}$ | 5.0E-01 | | [2] |
| $f1_{inh}$ | 1.0E-01 | | [2] |
| $f_c$ | 5.5E-01 | | [3] |
| $f_l$ | 1.5E-01 | | [3] |

References of Table 6 and

Table 7

[1] EPRI, 2002.

[2] ICRP, 1996.

[3] Coughtrey et al., 1983.

***Nirex***

Nirex divided the soil compartment into top and subsoil (Figure 3). Hydrological parameters have been selected base on irrigated, well-drained, lowland agricultural soil (

Table 8) [Thorne, 2003b].

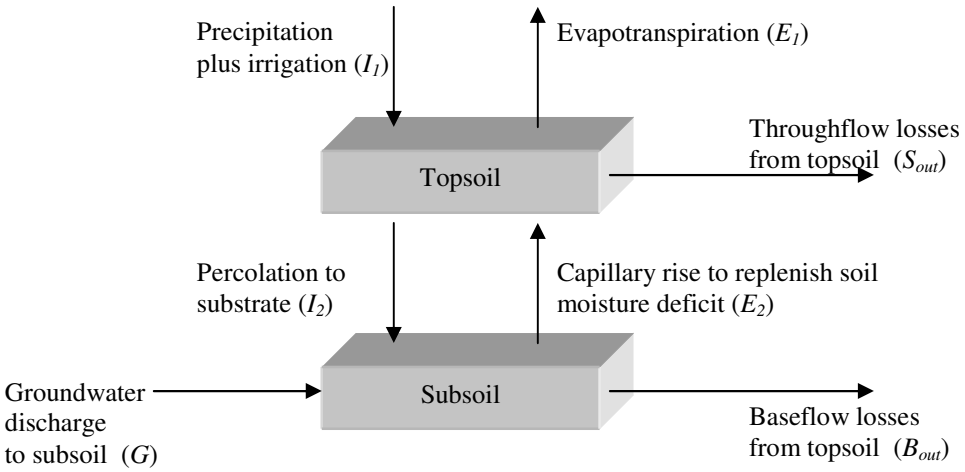


**Figure 3: Nirex model for well scenario**

**Table 8 : Hydrological parameters used by Nirex for the well scenario**

| Parameter | Units | Description | Value |
|---|---|---|---|
| $I_1$ | [m/y] | Precipitation plus irrigation | 8.0E-01 |
| $I_2$ | [m/y] | Percolation to substrate | 8.0E-01 |
| $E_1$ | [m/y] | Evapotranspiration | 2.5E-01 |
| $E_2$ | [m/y] | Capillary rise to replenish soil moisture deficit | 2.5E-01 |
| $S_{out}$ | [m/y] | Throughflow losses from topsoil | 0.0E+00 |
| $B_{out}$ | [m/y] | Baseflow losses from topsoil | 5.5E-01 |
| $G$ | [m/y] | Groundwater discharge to subsoil | 0.0E+00 |

Nirex prepared equilibrium concentrations of radionuclides in the soil as well as information on their dynamics. The former is evaluated by the “Nirex spread sheet”,

and the latter is calculated by integrating the mathematical equations that describes the single compartment soil model within an Excel spread sheet. As for the source term, the well water contains 1 Bq/L of each radionuclide with the same irrigation rate of 0.2 m/y used by other participants. Pb-210 arises only by ingrowth in the biosphere. Other specifications of the Nirex calculation are as follows:

- Crop soil contamination by soil splashing is not included, as soil consumption rates of animals and humans are specified directly, and double-counting should be avoided.

- The soil consumption rate of cattle was changed from 0.60 (recommenced value) to 0.70 kg(dw)/d. This is 1% of the fresh weight forage input. The breathing rate, occupancy and dust level for cattle are not represented, as inhalation of radionuclides by cattle is a minor pathway.

- The green and root vegetable human consumption rates were aggregated to give a total of 610 kg/y.

- The drinking water and resuspension pathways are considered and the well water is assumed to be used for human consumption at a rate of 0.6 $m^3$/y, as well as for irrigation.

***NUMO***

The NUMO model uses AMBER for calculation. AMBER is a flexible software tool that allows users to build their own dynamic compartmental models and to represent the migration and fate of contaminants in a system (for both surface and sub-surface environments). Radioactive and non-radioactive contaminants in solid, liquid and gaseous form can be considered. AMBER can be used to assess routine, accidental and long-term contaminant releases. Contaminants are assumed to be uniformly mixed in a series of compartments between which transfers can take place. A compartment is any specific part of the system being modelled [Walke et al, 2004].

NUMO uses mathematical expressions proposed by BIOMASS [IAEA, 2003]. The equation for percolation losses ($\lambda_I$) is given as an example:

$$\lambda_I = \frac{I}{R\,\theta_w\,d}$$

where:
$I$ is the irrigation rate [m/y],
$R$ is the retardation coefficient for the soil [-]
$\theta_w$ is the water filled porosity of the compartment [-] and
$d_w$ is the depth of the soil column [m].

The term of $R$ is calculated using the following equation:

$$R = 1 + \frac{(1-\theta_t)\rho K_d}{\theta_w}$$

where:
$\theta_t$ is the total porosity of the compartment [-],
$\rho$ is the grain density [kg/$m^3$].

$K_d$ is the sorption coefficient in the soil [$m^3$/kg] and
$\theta_w$ is the water filled porosity of the compartment [-].

***UKAEA***

UKAEA incorporates an unsaturated rock layer, which is situated below the soil layer (Figure 4).

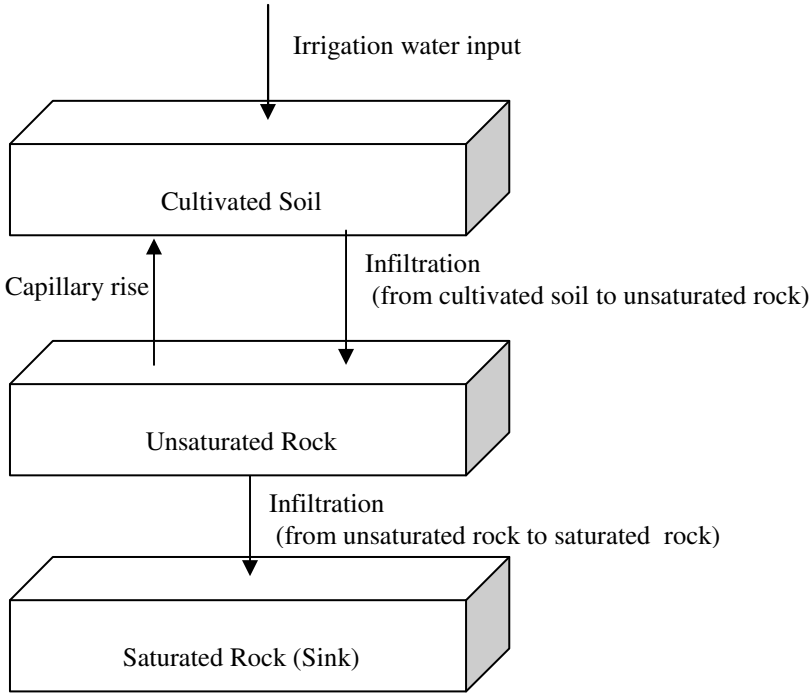


**Figure 4: UKAEA model used for the well scenario**

Both irrigation (infiltration) and capillary rise are considered to evaluate the concentration in the soil compartment. A general expression for advective transfer in ground water from compartment *i* to compartment *j* (written as $\lambda^{ij}{}_{w}$ [1/y]) has been applied.

$$\lambda^{ij}{}_{w} = \frac{Q^{ij}\left(1 + S^{i} K_{d}{}^{i}\right)}{\kappa^{i}}$$

where:
$Q^{ij}$ is the appropriate flux of water between compartments *i* and *j* [$m^3$/y],
$S^{i}$ is the concentration of suspended solids and colloids in liquid phase [kg/$m^3$],
$K_d{}^{i}$ is the distribution coefficient [$m^3$/kg].

The term $\kappa^{i}$ (the capacity of the compartment *i*, $m^3$) is calculated using following equation:

$$\kappa = \kappa_L + \kappa_S + \kappa_C$$

where:

$$\kappa_L = V\varepsilon\theta_{flow} \;,\; \kappa_S = V\varepsilon\beta\rho(1-\theta_{total})K_d \;,\; \kappa_C = V\varepsilon\theta_{flow}K_d S$$

and:
$V$ is the volume of the compartment [$m^3$],
$\varepsilon$ is the degree of saturation [-],
$\theta_{flow}$ is the flowing porosity [-],

$\beta$ is the fraction of solid in contact with flowing liquid [-],
$\rho$ is the grain density [kg/m$^3$],
$\theta_{total}$ is the total porosity [-],
$K_d$ is the distribution coefficient between solid and liquid [m$^3$/kg], and
$S$ is the concentration of suspended solids and colloids in liquid phase [kg/m$^3$].

Parameters necessary for the mathematical model are given in Table 9 and Table 10. Radionuclide specific data for Po-210 are given in

Table 11.

**Table 9: Compartment properties in the UKAEA calculation**

| | Soil | Unsaturated rock | Saturated rock | Remarks (suggested value for soil by task leader) |
|---|---|---|---|---|
| Depth of the compartment [m] | 3.0E-01 | 2.0E+00 | 1.3E+01 | 3.0E-01 |
| Volume of the compartment [m$^3$] | 3.0E-01 | 2.0E+00 | 1.3E+01 | - |
| Total porosity [-] | 5.0E-01 | 1.5E-01 | 4.0E-02 | 5.0E-01 |
| Flow porosity [-] | 5.0E-01 | 1.5E-01 | 4.0E-02 | - |
| Grain density [kg/m$^3$] | 2.65E+03 | 2.4E+03 | 2.4E+03 | 2.65E+03 |
| Degree of saturation [-] | 8.7E-01 | 7.5E-01 | 7.5E-01 | 6.0E-01 |
| Fraction of solid in contact with flowing liquid [-] | 1.0E+00 | 1.0E+00 | 1.0E+00 | - |
| Concentration of suspended solids and colloids in liquid phase [kg/m$^3$] | 0.0E+00 | 0.0E+00 | 1.0E-05 | - |
| Distribution coefficient between solid and liquid [m$^3$/kg] | | | | |
| Cl-36 | 5.8E-03 | 5.8E-03 | 5.8E-03 | 5.8E-03 |
| Se-79 | 7.4E-01 | 7.4E-01 | 7.4E-01 | 7.4E-01 |
| Tc-99 | 1.0E-04 | 1.0E-03 | 1.0E-02 | 1.0E-04 |
| I-129 | 5.0E-03 | 5.0E-03 | 5.0E-03 | 5.0E-03 |
| Np-237 | 3.0E-02 | 3.0E-02 | 3.0E-02 | 3.0E-02 |
| Ra-226 | 5.0E+00 | 5.0E+00 | 5.0E+00 | 5.0E+00 |
| Pb-210 | 5.4E-01 | 5.4E-01 | 5.4E-01 | 5.4E-01 |
| Po-210 | 1.5E-01 | 1.5E-01 | 1.5E-01 | - |

**Table 10: Hydrological parameters as used in the UKAEA calculations**

| Parameters | Value [m/y] | Remarks (suggested value by task leader [m/y]) |
|---|---|---|
| Irrigation rate to soil | 2.0E-01 | 2.0E-01 |
| Infiltration rate from soil to unsaturated rock | 1.0E-01 | 1.0E-01 |
| Infiltration rate from saturated rock to unsaturated rock | 1.0E-01 | - |
| Capillary rise from unsaturated rock to soil | 1.08E-01 | - |

**Table 11: Radionuclide dependent parameters of Po-210 as used in the UKAEA calculations**

| Parameter | Value | Unit |
|---|---|---|
| Decay constant | 1.83E+00 | [1/y] |
| Ingestion dose coefficient | 1.2E-06 | [Sv/Bq] |
| External dose factor | 1.05E-18 | [(Sv/h)/(Bq/m$^3$)] |
| Plant concentration factor | | [(Bq/kg)/(Bq/kg)] |
| - root veg | 2.0E-04 | |
| - green veg | 2.0E-04 | |
| - pasture | 2.0E-04 | |
| Transfer factor to cow products from ingestion | | |
| - meat | 1.0E-02 | [d/kg] |
| - milk | 1.0E-02 | [d/L] |
| - liver | 5.0E-01 | [d/kg] |

# 2. RESULTS OF THE WELL SCENARIO

BNFL, UKAEA, EPRI, NUMO, EDF, Nirex, ANDRA and Aleksandria Sciences (AlekSci) participated in the calculation exercises for the well scenario.

In the first part of this section, activities of radionuclides in the soil compartment calculated by participants are shown as a function of time (Figure 5 through to Figure 15). In the second part focus will be given to equilibrium values[1].

## 2.1 Evolution with time

### 2.1.1 Chlorine-36

The results for Cl-36 (Figure 5) can be categorised into three groups. Higher soil concentrations were modelled by UKAEA, AlekSci, NUMO and ANDRA. BNFL and EPRI obtained lower results with low equilibration times. EDF and Nirex take an intermediate position (i.e. equilibrium reached in about 100 years). Interpretation of the results of EDF have to take into the consideration that seasonal change and smaller irrigation rates were used (§0). Higher concentrations for summer and lower for winter periods are related to summer irrigation (Table 5) and higher percolation losses during the cold period. As for the result obtained by Nirex, the net flow rate from topsoil to subsoil and discharge baseflow loss from the sub soil has been set as 0.55m/y (§0). This larger flow rate makes the concentration in the topsoil lower compared to most other participants (UKAEA, AlekSci, NUMO and ANDRA).

Lower concentrations obtained by BNFL and EPRI are related to their consideration of cropping loss (see high plant concentration factor for Cl-36). Annual crop yield was identical for both participants (3 kg/($m^2$y)) except for the higher yield value used by EPRI for grass (5 kg/($m^2$y)). The use of different yield parameter values is one possible cause for the slightly lower values obtained by EPRI in comparison with BNFL. Another potential reason will be discussed later (§3.1.2).

Figure 6 shows the result using a linear scale with focus on the first 1500 years. ANDRA and NUMO obtain an equilibrium concentration at around 100 years, AlekSci and UKAEA require longer equilibration times. The higher concentrations for Cl-36, modelled by UKAEA (brown curve in Figure 5) is related to the second (unsaturated) soil layer located below the surface soil layer. Radionuclides lost from the soil system are in part stored in the lower layer and reintroduced into the upper layer via capillary rise. UKAEA selected 0.108 m/y (higher than the prescribed infiltration rate of 0.1 m/y). This additional radionuclide flux related to capillary rise becomes significant after an irrigation period of 100 years. This argument could also be applied to the result of AlekSci.

1 EDF included seasonal changes of the irrigation rate and prepared monthly results of up to 1364 years (16382 months) for Se-79, and 133 years (1800 months) for the other radionuclides.

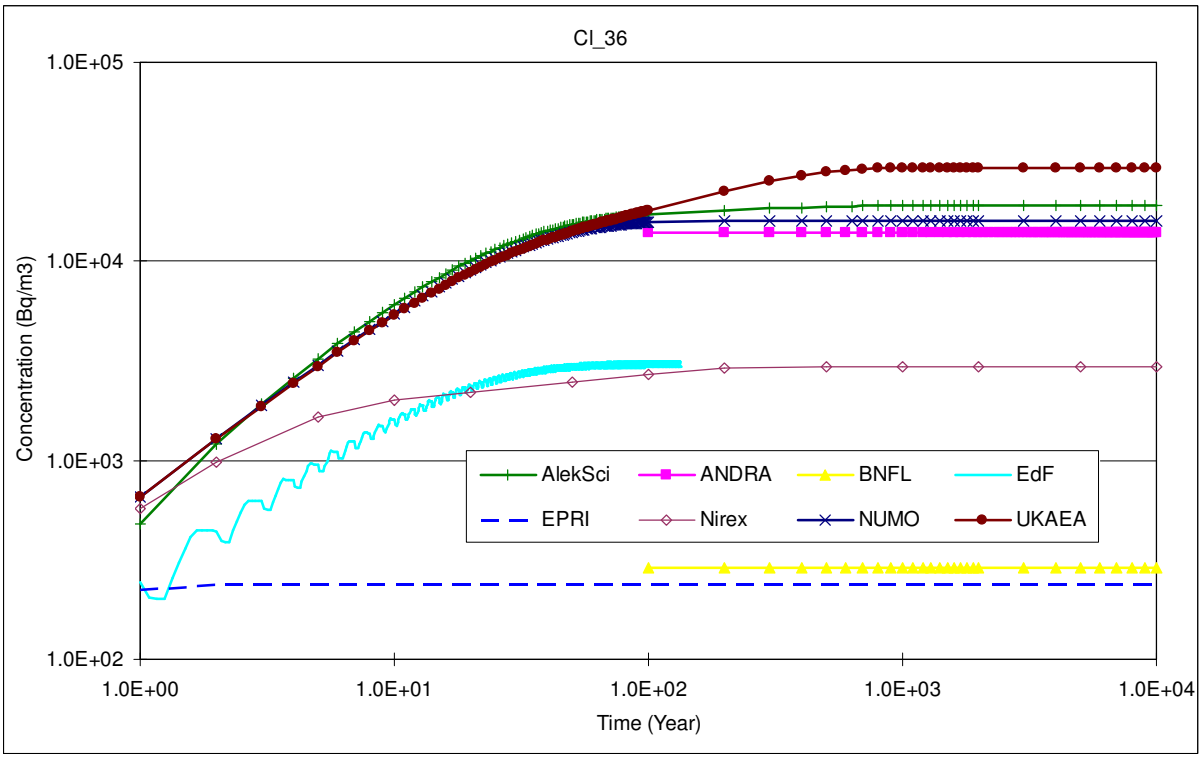


**Figure 5: Cl-36 concentration in the soil [Bq/m$^3$] as a function of time as modelled by the different participants (log-log scale)**

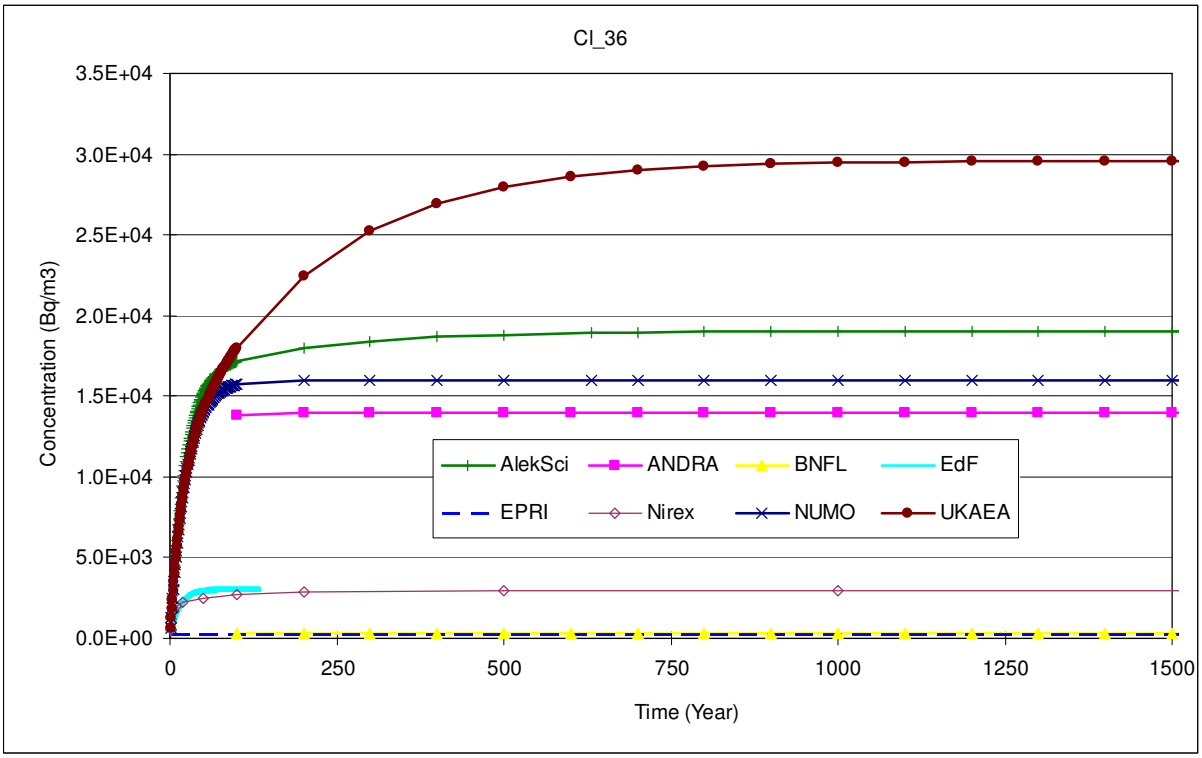


**Figure 6: Cl-36 concentration in the soil [Bq/m$^3$] as a function of time as modelled by the different participants (linear scale)**

### 2.1.2 Selenium-79

Comparison of modelled soil activities for Se-79 (Figure 7) indicates the close similarity of results obtained by UKAEA and NUMO. Their activities are somewhat higher than those obtained by ANDRA, BNFL, EPRI and AlekSci. As was seen for Cl-36, Nirex and EDF model lower soil activities. Smaller irrigation rates of EDF and larger water flow rates from the soil compartment of Nirex are the most probable reasons, as discussed in the previous paragraph.

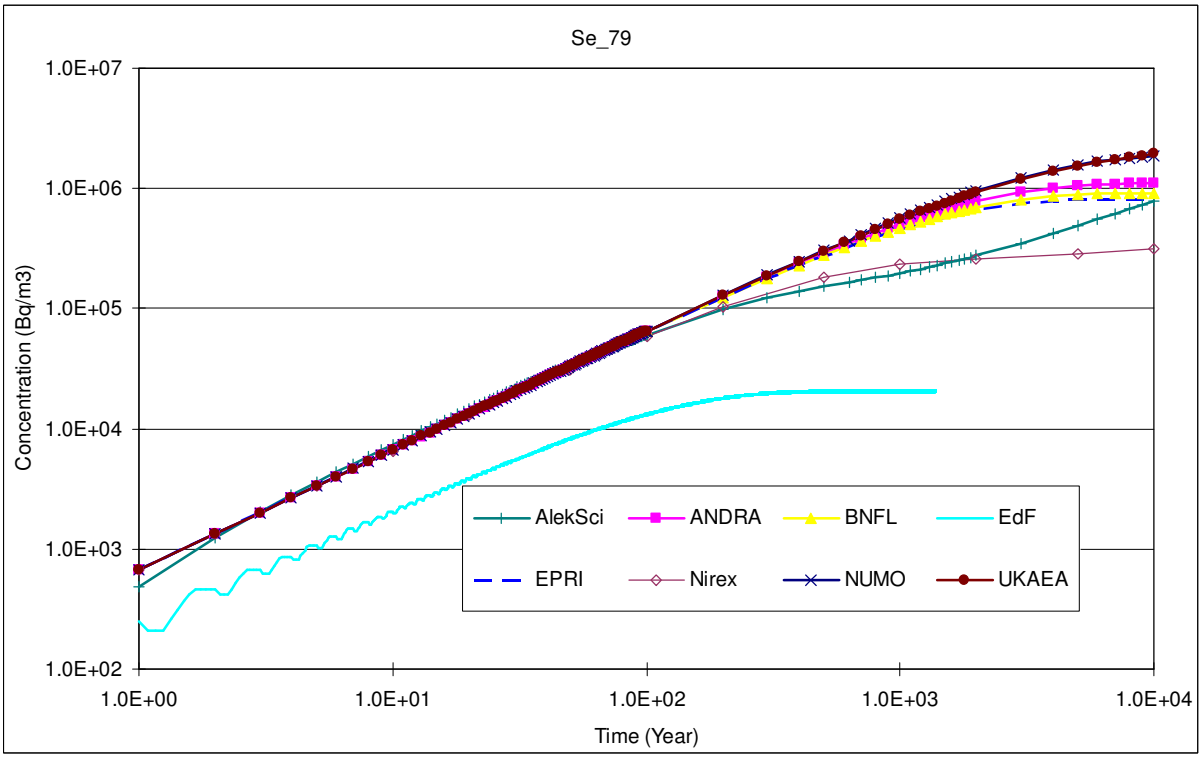


**Figure 7: Se-79 concentration in the soil [Bq/m$^3$] as a function of time as modelled by the different participants (log-log scale)**

The result for Se-79 plotted on a linear scale is available in Figure 8. Results obtained by ANDRA, BNFL and EPRI reach their equilibrium concentration after about 8,000 years. NUMO is getting closer to its equilibrium after 10,000 years. For AlekSci and UKAEA, and to some extent for Nirex as well, results are still increasing at the end of calculation due to the transfer from the lower soil layer.

BNFL and EPRI who modelled cropping obtain lower concentrations. The impact is smaller compared to Cl-36 because of the smaller plant concentration factors for Se-79 (more quantitative discussion about the effects of cropping is given §3.1.1).

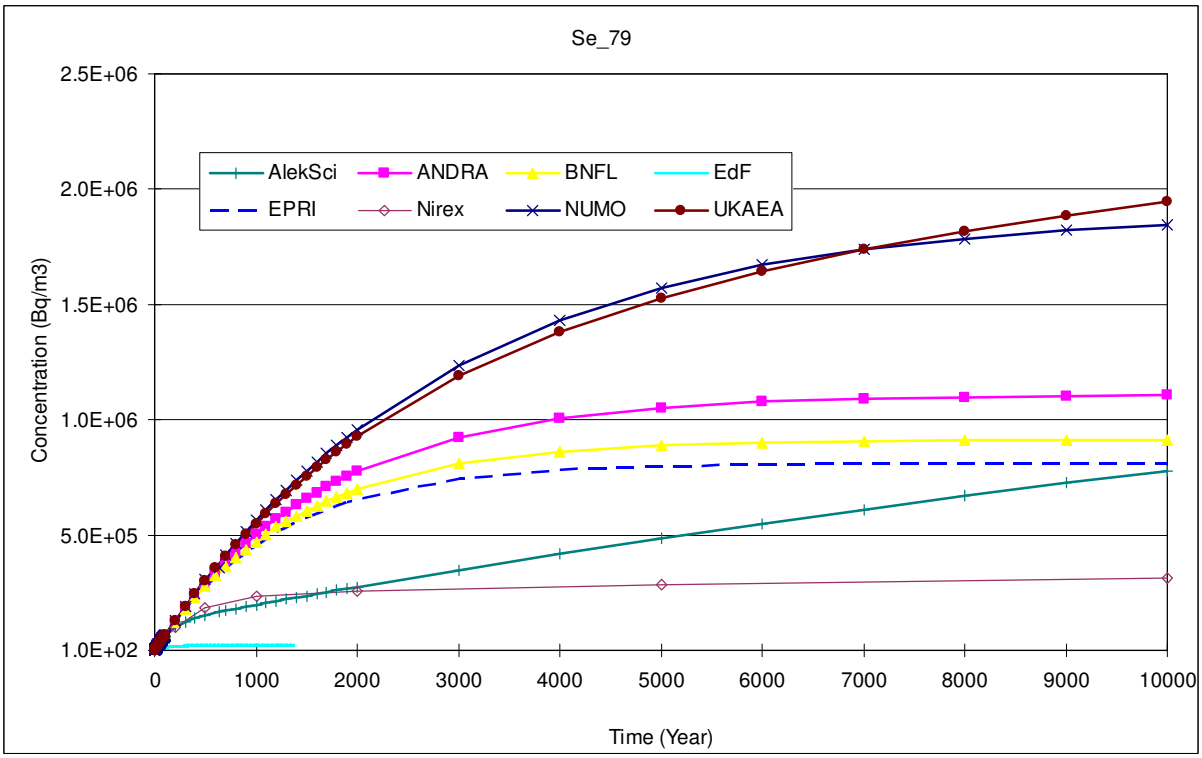


**Figure 8: Se-79 concentration in the soil (Bq/m$^3$) as a function of time as modelled by the different participants (double linear scale)**

### 2.1.3 Technetium-99

Equilibrium between input flux and losses is reached after 10 years (Figure 9). The higher equilibration periods of 20 years and 100 years, obtained by Nirex and UKAEA are related to upward fluxes from the lower soil compartment.

In the EDF model "equilibrium" is continuously disturbed, because periods of radionuclide addition (irrigation period) are followed by periods of enhanced lixiviation (seasonal cold periods with enhanced precipitation, reduced evaporation and transpiration, thus enhanced percolation). For Tc-99 this situation is particularly obvious, because Tc-99 behaviour is modelled using the lowest of all Kd values (1.0E-04 m$^3$/kg). The seasonal perturbation between August and March, as modelled by EDF seen throughout the entire calculation period (Figure 10), yields a summer soil activity enhanced by a factor of 2.6 compared to the winter activity.

The soil modelled by UKAEA requires a longer time to reach equilibrium due to the presence of a lower soil layer and the consideration of capillary rise. This "recycling" of radionuclides into the upper soil compartment explains the higher activities obtained by UKAEA.

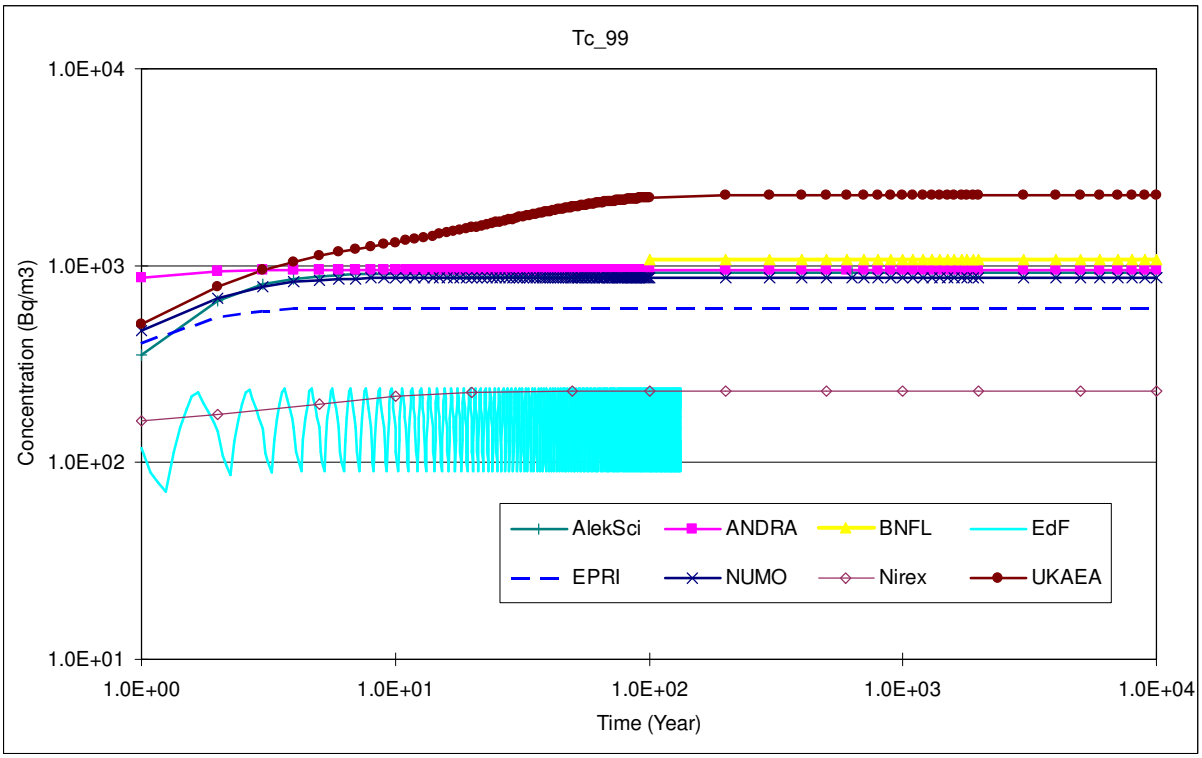


**Figure 9: Tc-99 concentration in the soil [Bq/m$^3$] as a function of time as modelled by the different participants (log-log scale)**

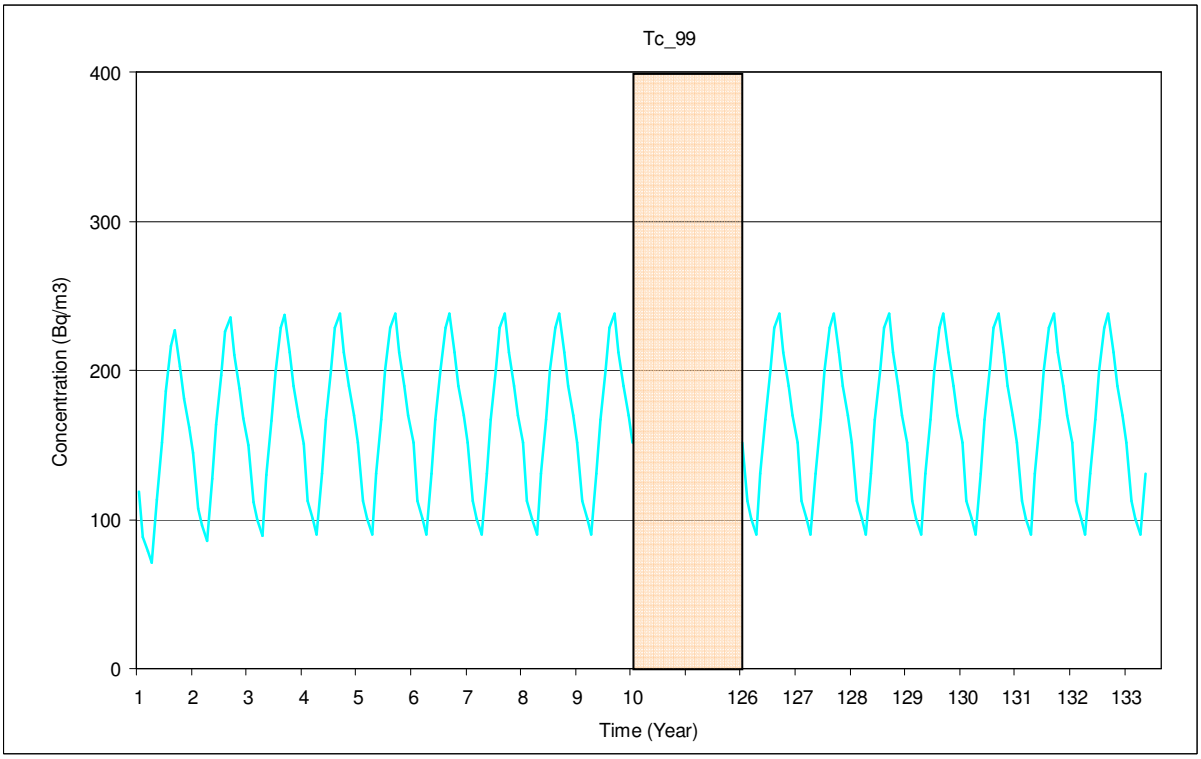


**Figure 10: Tc-99 concentration in the soil [Bq/m$^3$] as a function of time as modelled by EDF (linear scale)**

### 2.1.4 Iodine-129 and Neptunium-237

Activities of I-129 and Np-237 in the soil follow similar trends (Figure 11, Figure 12 and Figure 13). I-129 activities reach equilibrium after about 200 years and 1000 years in the Nirex model and UKAEA model respectively, and after 100 years in the other models. Np-237 reaches equilibrium significantly later (several thousands years for AlekSci and UKAEA and around 1000 years for the others).

The consideration of a lower soil layer, as modelled by UKAEA and AlekSci, results in higher equilibrium activities. Results modelled by EDF and Nirex are lower as a consequence of the lower irrigation rates (and possibly higher percolation losses) of EDF and larger water loss rate from the soil compartment of Nirex. The other participants (ANDRA, BNFL, EPRI and NUMO) used comparable model approaches.

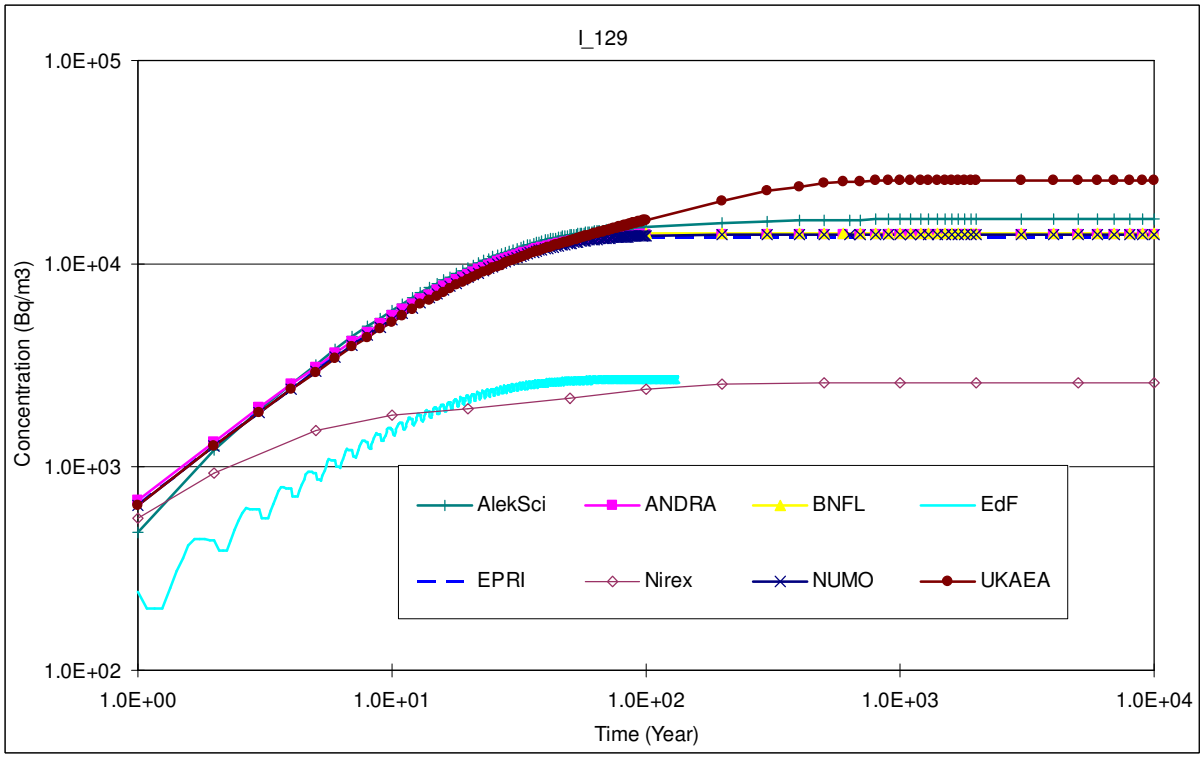


**Figure 11: I-129 concentration in the soil [Bq/m$^3$] as a function of time as modelled by the different participants (log-log scale)**

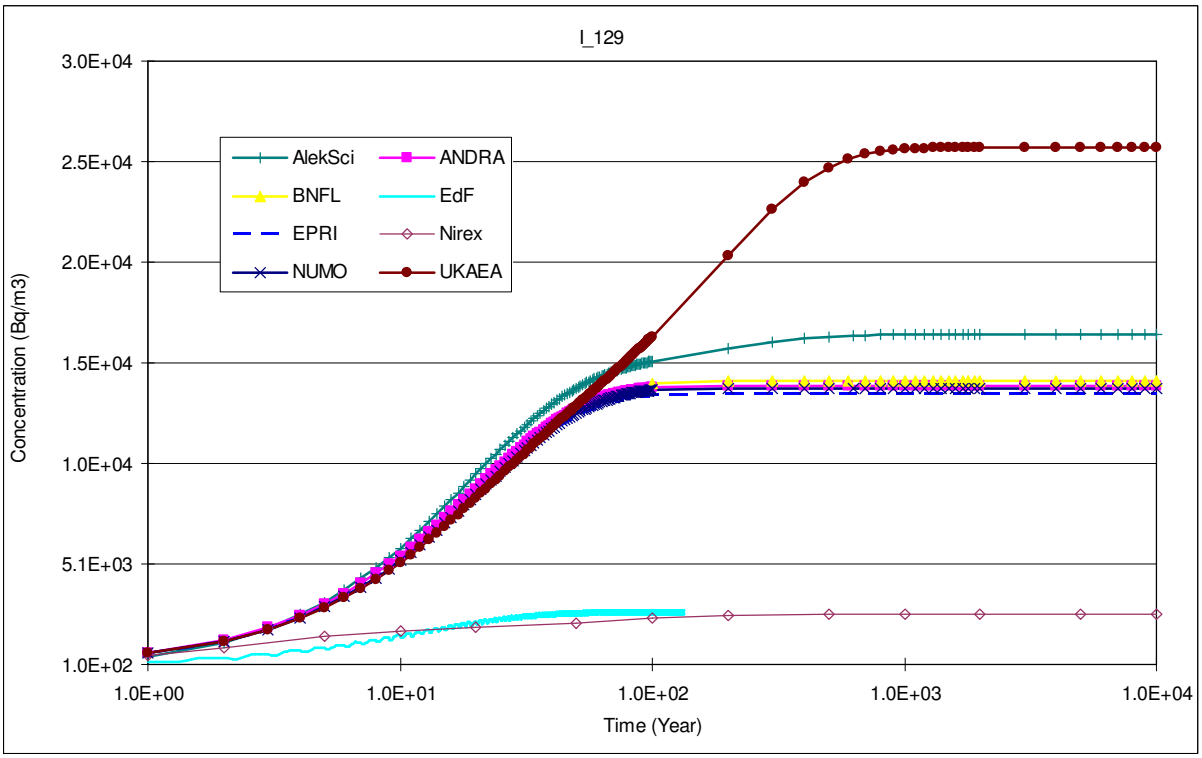


**Figure 12: I-129 concentration in the soil [Bq/m$^3$] as a function of time as modelled by the different participants (linear scale)**

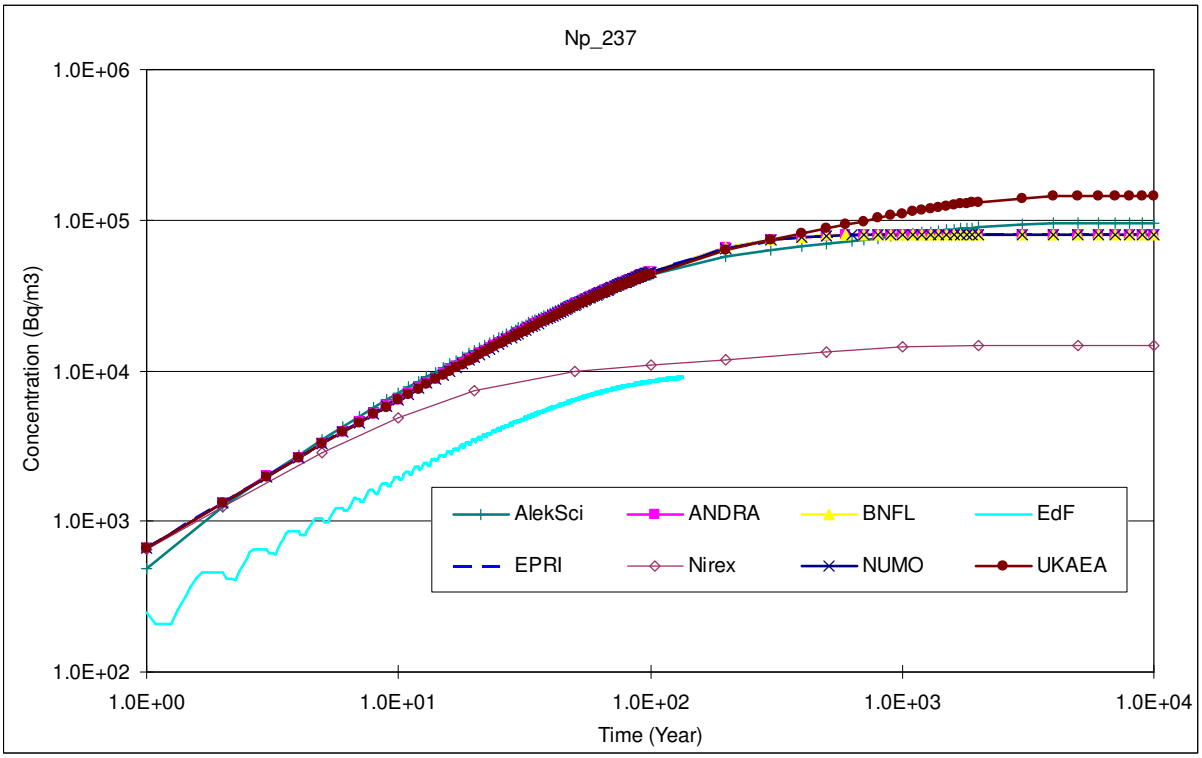


**Figure 13: Np-237 concentration in the soil [Bq/m$^3$] as a function of time as modelled by the different participants (linear scale)**

### 2.1.5 Radium-226 and its daughters

Results for Ra-226 (Figure 14) were calculated together with those of their daughters (Pb-210 and Po-210 shown in Figure 15). Different model approaches were applied by AlekSci and EDF (two layer soil model and monthly irrigations, respectively, see above), both resulting in lower soil activities (Figure 14). The high sorption coefficient of Ra-226 (5 $m^3$/kg) explains the long time period of 8,000 years that is necessary to reach equilibrium. The result of EDF is again lowest among the participants partly because of the smaller irrigation rate and partly because they terminated the calculation during the period when radionuclides were still accumulating in the soil.

For Ra-226, the Nirex result is comparable to those of other participants. This indicates that for Ra-226 which has larger radioactive decay constant and Kd value, the loss of nuclides from the soil compartment is dominated by radioactive decay.

The daughter radionuclides Pb-210 and Po-210 are not part of the contamination at the source. Their appearance in the biosphere is related to ingrowth from the decaying parent, Ra-226. As shown in Figure 15 secular equilibrium is reached at all times (identical activities).

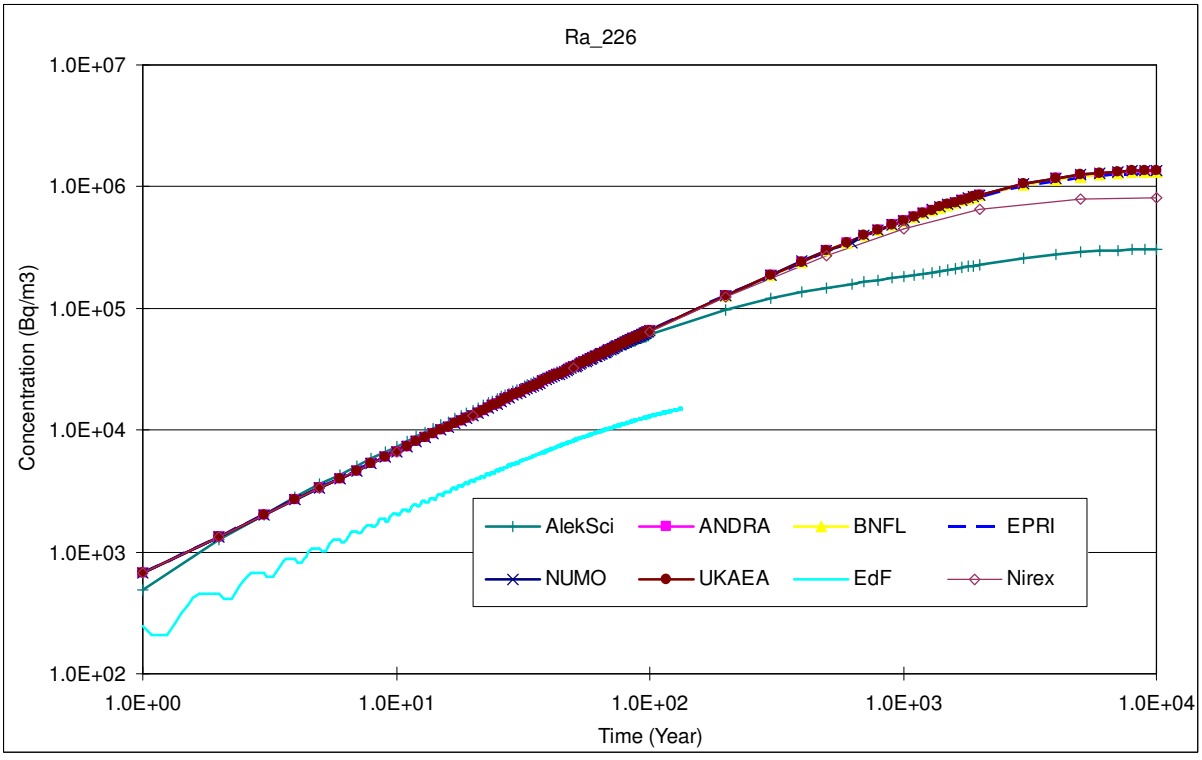


**Figure 14: Ra-226 concentration in the soil [Bq/$m^3$] as a function of time as modelled by the different participants (log-log scale)**

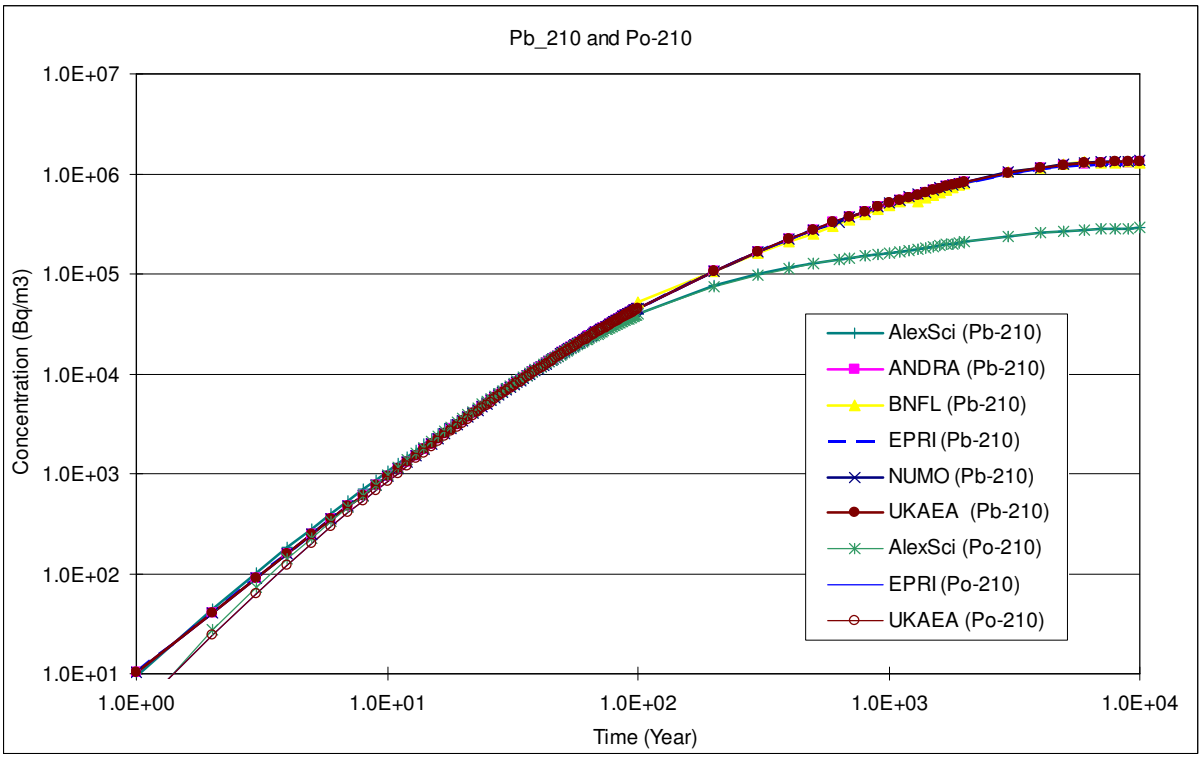


**Figure 15: Pb-210 and Po-210 concentration in the soil [Bq/m$^3$] as a function of time as modelled by the different participants (log-log scale)**

## 2.2 Radionuclide concentrations in the soil at 10,000 years

The radionuclide concentration in the soil modelled for a continuous period of contamination of 10,000 years are tabulated (

Table 12) and illustrated graphically (Figure 16). Note that EDF terminated their calculation after 1364 years for Se-79 and after 133 years for the other radionuclides. Results of EDF shown in

Table 12 and Figure 16 are those given at the end point of their calculations.

In the Nirex calculation, radionuclide concentrations in the lower and upper soil layer are identical for Cl-36, Tc-99, I-129 and Np-237. But for some shorter-lived highly adsorbed radionuclides, radioactive decay is sufficient to reduce subsoil concentration compared to the topsoil. The results obtained for Se-79 for which slightly lower concentrations were obtained in the lower soil compartment and for Ra-226 (and Pb-210 that is in secular equilibrium) for which differences are larger than 1 order of magnitude, serve as illustrations. It is worthwhile pointing out that, for those radionuclides for which Nirex calculated identical concentrations for the top and lower soil (except for Np-237), Nirex has consistently slightly lower concentrations compared to EDF, but the values are very similar. On the other hand for radionuclides with significantly higher modelled top soil concentrations, Nirex obtained intermediate (Se-79) or compatible concentrations (Ra-226) compared to the others. This tendency could be considered in more detail in the future with additional information on hydrological parameters selected by Nirex for their assessment.

**Table 12: Radionuclide concentrations in soil at 10,000 years (Bq/m$^3$)**

| | Cl-36 | Se-79 | Tc-99 | I-129 | Np-237 | Ra-226 | Pb-210 | Po-210 |
|---|---|---|---|---|---|---|---|---|
| AlekSci | 1.9E+04 | 7.8E+05 | 9.2E+02 | 1.7E+04 | 9.6E+04 | 3.1E+05 | 2.9E+05 | 2.9E+05 |
| ANDRA | 1.4E+04 | 1.1E+06 | 9.5E+02 | 1.4E+04 | 8.0E+04 | 1.3E+06 | 1.3E+06 | - |
| BNFL | 2.9E+02 | 9.1E+05 | 1.1E+03 | 1.4E+04 | 8.1E+04 | 1.3E+06 | 1.3E+06 | - |
| EDF | 3.1E+03 | 2.1E+04 | 2.4E+02 | 2.8E+03 | 9.1E+03 | 1.5E+04 | - | - |
| EPRI | 2.4E+02 | 8.1E+05 | 6.1E+02 | 1.4E+04 | 8.0E+04 | 1.3E+06 | 1.3E+06 | 1.3E+06 |
| Nirex (Topsoil) | 3.0E+03 | 3.5E+05 | 2.3E+02 | 2.6E+03 | 1.5E+04 | 8.0E+05 | 7.2E+05 | - |
| Nirex (Subsoil) | 3.0E+03 | 3.2E+05 | 2.3E+02 | 2.6E+03 | 1.5E+04 | 4.3E+04 | 4.7E+04 | - |
| NUMO | 1.6E+04 | 1.8E+06 | 8.6E+02 | 1.4E+04 | 8.0E+04 | 1.4E+06 | 1.3E+06 | - |
| UKAEA | 3.0E+04 | 1.9E+06 | 2.3E+03 | 2.6E+04 | 1.5E+05 | 1.4E+06 | 1.3E+06 | 1.3E+06 |

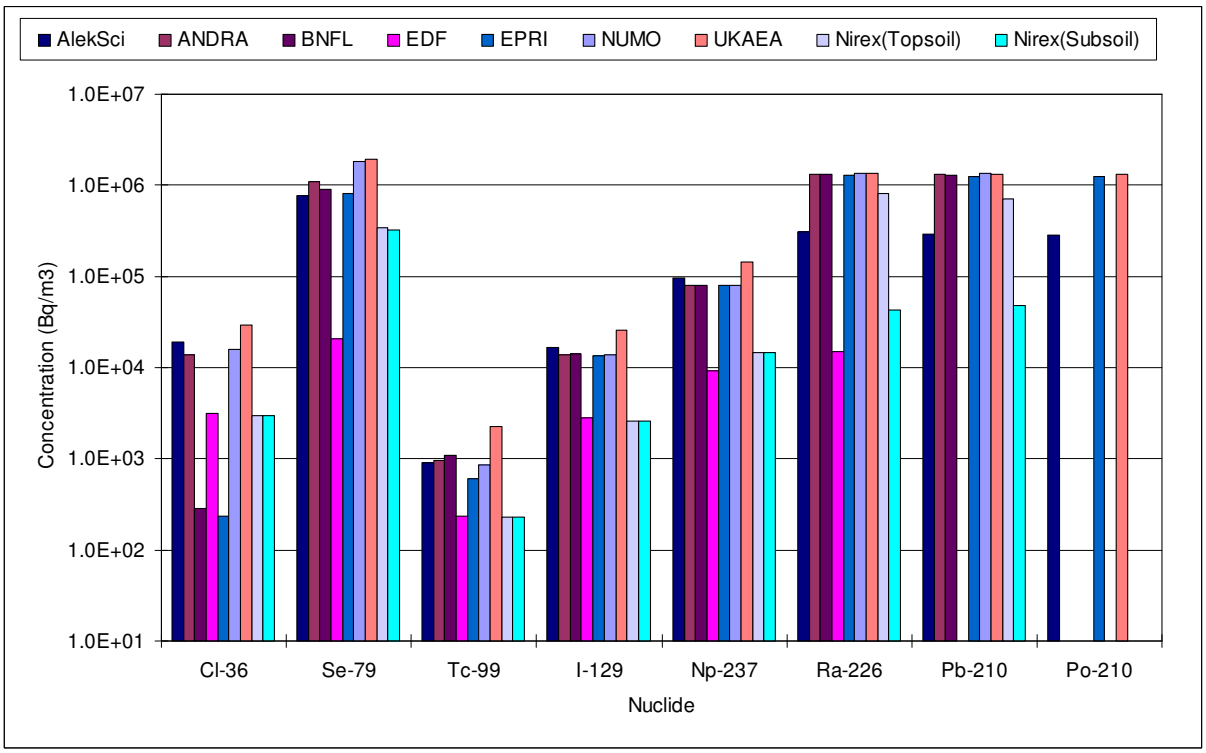


**Figure 16: Radionuclide concentrations in the soil after 10,000 years of accumulation**

# 3. DISCUSSION

## 3.1 Radionuclide concentration in the soil compartment

### 3.1.1 Radionuclide losses due to cropping

The influence of cropping can be illustrated by comparing loss rates determined by BNFL, as a representative of the modellers who included cropping losses and NUMO, as a representative of those who did not (

Table 13). Rates of all considered loss processes are given including radioactive decay.

For Cl-36 the cropping loss rates are particularly important because of high concentration factors for all plants (300 (Bq/kg(fw))/(Bq/kg(dw))), Cropping losses exceed percolation losses, in spite of the fact that these are also rather high related to the low sorption coefficient for the soil. Furthermore the radioactive decay constant is low. Percolation losses were considered by all participants. Differences are minute, allowing a quantification of the differences caused by the consideration of cropping losses. The equilibrium concentration in the soil is proportional to $S/\lambda$, where $S$ [Bq/y] is the source term and $\lambda$ [1/y] the total loss rate from the soil compartment. In the BNFL model which considers cropping losses overall losses are about two orders of magnitude larger than percolation losses. This enhancement of soil losses yields equilibrium concentrations that are about two orders of magnitude smaller than those calculated without the consideration of cropping losses.

The influence of cropping is also relevant for Se-79 and Tc-99 (

Table 13) but with less significance than what was observed for Cl-36. For Se-79, BNFL and EPRI obtained considerably lower concentrations than UKAEA and NUMO, and slightly lower than ANDRA (Figure 7 and Figure 8), as a consequence of the consideration of cropping losses. For Tc-99, the contribution of cropping to the total loss rate of BNFL is about 13%, which is much smaller than that for Cl-36 and Se-79. As a result, EPRI obtained lower concentrations, but the difference between EPRI and other participants is less significant compared to Cl-36 and Se-79. The slightly higher concentrations of BNFL compared to NUMO that are not related to cropping will be discussed in the next section.

**Table 13: Summary of loss rates calculated by BNFL and NUMO modelling for well scenario**

| | decay [1/y] | cropping loss [1/y] | percolation or leaching loss [1/y] | | total loss [1/y] | |
|---|---|---|---|---|---|---|
| | BNFL/NUMO | BNFL | BNFL | NUMO | BNFL | NUMO |
| Cl-36 | 2.30E-06 | 2.26E+00 | 4.07E-02 | 4.17E-02 | 2.30E+00 | 4.17E-02 |
| Se-79 | 1.10E-05 | 3.77E-04 | 3.40E-04 | 3.40E-04 | 7.28E-04 | 3.51E-04 |
| Tc-99 | 3.30E-06 | 7.55E-02 | 5.27E-01 | 7.71E-01 | 6.02E-01 | 7.71E-01 |
| I-129 | 4.40E-08 | 2.26E-04 | 4.68E-02 | 4.81E-02 | 4.70E-02 | 4.81E-02 |
| Np-237 | 3.20E-07 | 2.26E-05 | 8.28E-03 | 8.32E-03 | 8.30E-03 | 8.32E-03 |
| Ra-226 | 4.30E-04 | 2.26E-05 | 5.03E-05 | 5.03E-05 | 5.03E-04 | 4.80E-04 |
| Pb-210 | 3.10E-02 | 7.55E-06 | 4.66E-04 | 4.66E-04 | 3.15E-02 | 3.15E-02 |

### 3.1.2 Modelling of percolation (leaching) losses

Divergence in modelling percolation losses of the soil compartment is the second major reason for differences found in the intercomparison. The details of these differences are given by comparing the approaches of BNFL with those of NUMO.

Different equations are applied to evaluate percolation loss rates. Both participants base their calculations on an equation used in BIOMASS ERB 2A [IAEA, 2003]. As mentioned in §1.3.2, BNFL modified the original equation by replacing the water filled porosity of the soil with the total porosity.

$$\lambda_I = \frac{I}{R\theta_w d} \quad \text{,where} \quad R = 1 + \frac{(1-\theta_t)\rho K_d}{\theta_w}$$

This equation can be rewritten as follows:

$$\lambda_I = \frac{I}{\theta_w d\left[1 + \frac{(1-\theta_t)\rho K_d}{\theta_w}\right]} = \frac{I}{d(\theta_w + (1-\theta_t)\rho K_d)} \quad (equation\ 1,\ for\ NUMO)$$

$$= \frac{I}{d(\theta_t + (1-\theta_t)\rho K_d)} \quad (equation\ 2,\ for\ BNFL)$$

The difference between the two approaches used by BNFL and NUMO becomes significant as $K_d$ becomes smaller. Actually, as shown in

Table 13, for a Kd of 1.0E-04 $m^3$/kg (Tc-99) the above-mentioned equations yield for the percolation loss rate $\lambda_I$ values of 5.27E-01 (equation 2, BNFL) or 7.71E-01 (equation 1, NUMO), respectively.

The difference in percolation losses as a function of Kd modelled with equation 1 and equation 2 (Figure 17) becomes apparent for Kd values smaller than 1.0E-03 $m^3$/kg as is the case of Tc-99. For radionuclides with similar low Kd values comparable deviations are to be expected.

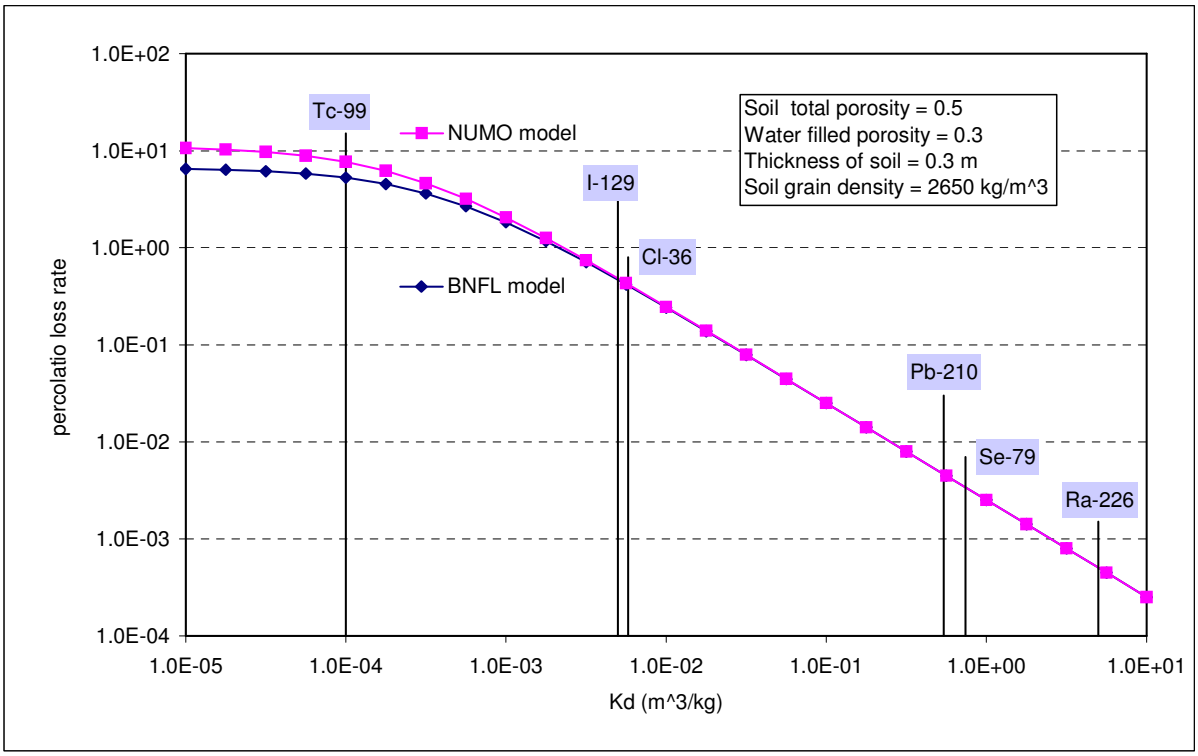


**Figure 17: Percolation loss rates as a function of soil Kd modelled using equation 1 (i.e. BNFL) and equation 2 (NUMO, ANDRA and others)**

### 3.1.3 Seasonal changes

Models designed for long term risk assessment such as those used for high level nuclear waste feasibility studies base all of their calculations on yearly averages, thus not considering seasonal changes. The model developed by EDF is primarily designed to evaluate the impact of nuclear reactor emissions. Here seasonal changes are accounted for. This has a significant impact on the definition of irrigation rates not only because EDF irrigated only during the summer season, but also the total amount of irrigation applied during one year was 0.075 m, a factor of 0.38 times smaller than the amount applied by all other participants (Table 5). This means that a correct comparison of results obtained by EDF requires correction by a factor of 2.66 (=irrigation rate of BIOPROTA/irrigation rate of EDF = 0.2/0.075). (see Appendix A on the assumption of the linear relationship between irrigation and soil concentration). Such a correction has been applied for Se-79 (Figure 18).

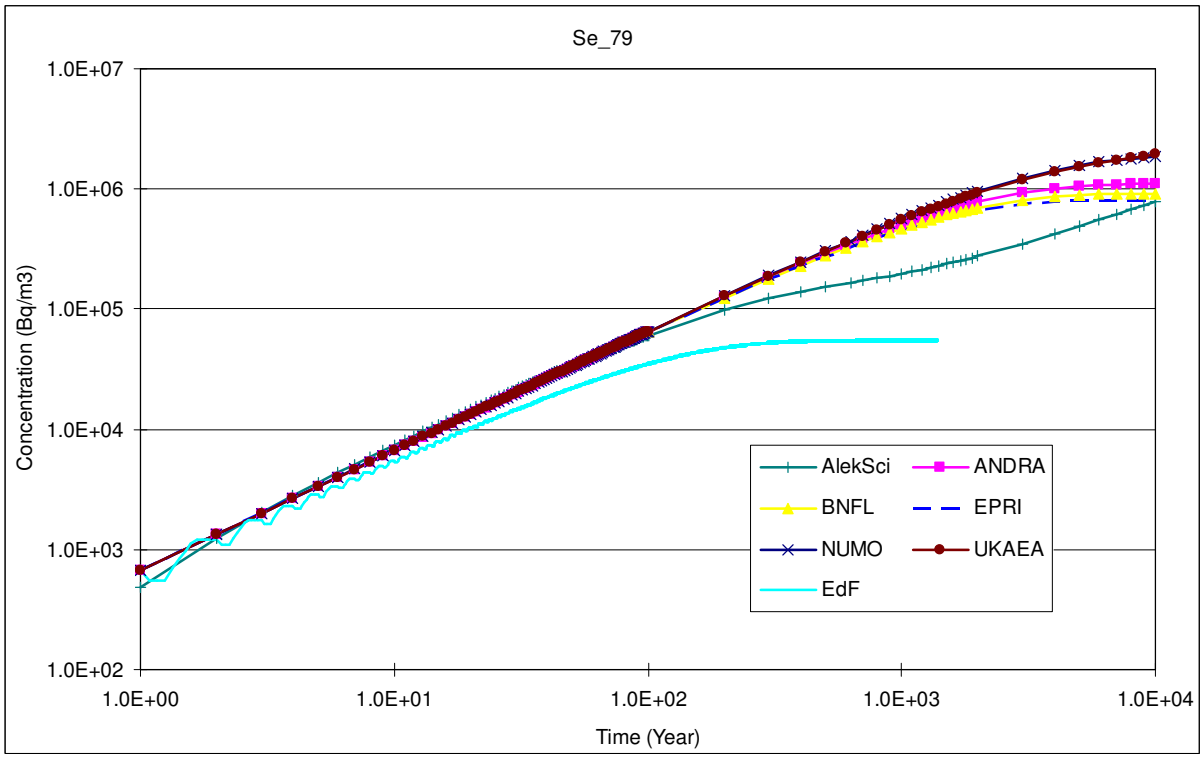


**Figure 18: Irrigation-rate corrected soil concentration of EDF for Se-79 [Bq/m$^3$] compared with results obtained by other participants (log-log scale)**

For the first 10 to 20 years the irrigation-rate corrected soil concentration for EDF is comparable with results obtained by other participants. Deviations still remain and become obvious during later stages of the system development (between 1 to 2 orders of magnitude lower than other participants after 100 years of accumulation), This tendency is commonly seen for all radionuclides (see Appendix B).

For a single soil compartment system with an initial activity of zero and a constant source term the soil activity can be approximated with the following analytical expression (see Appendix A):

$$N(t) = \frac{S}{\lambda}\left[1 - \exp(-\lambda t)\right]$$
$$\cong \begin{cases} S \cdot t & (for\ small\ t) \\ S/\lambda & (for\ t = \infty) \end{cases}$$

with

*N(t)* the activity of radionuclides in the soil compartment [Bq/m$^3$],

*S(t)* the external source term [Bq/y] and

$\lambda$ the total loss rate from the soil compartment [1/y].

For the interpretation of the results obtained by EDF this would mean that during the first period of accumulation the system is dominated by the input (comparability of results with other participants, Figure 18), but during the remaining period, loss rates become dominant (with $S/\lambda$ as the equilibrium concentration). It can thus be concluded that EDF applied a total effective loss rate which is superior to the value used by other participants. Potentially this difference between EDF and other participants may be a consequence of their consideration of seasonal change. A detailed look at the parameterisation of the water balance of the soil compartment should be given more detailed consideration in the future.

## 3.2 Human dose

Concerning the calculation of the human dose, some participants considered additional or different exposure pathways than those given in the specifications (§1.3). As shown in

Table 14, Nirex and EDF considered pathways that were not specified, Nirex the drinking water and resuspension pathways, EDF the drinking water pathway. Furthermore, EDF and Nirex categorised plants and animal products in a different way compared to the other participants.

**Table 14: Summary of exposure pathways modelled**

| Organization | Ingestion of plants | Ingestion of animal product | Others |
|---|---|---|---|
| AlekSci, ANDRA, BNFL, EPRI, NUMO and UKAEA | - Root vegetable<br>- Green vegetable | - Meat<br>- Milk<br>- Liver | - Soil ingestion<br>- External irradiation |
| EDF | - Vegetable | - Meat<br>- Milk | - Drinking water |
| Nirex | - Plant ingestion | - Animal products | - Soil ingestion<br>- External irradiation<br>- Resuspension<br>- Drinking water |

Total human doses after 10,000 years of continuous contamination have been calculated by all participants (Figure 19). Note that EDF carried out their calculations for shorter periods. Discrepancies do not exceed 1 order of magnitude for most radionuclides. Cl-36 forms an exception for which the difference between the highest and lowest modelled values is of 3 orders of magnitude.

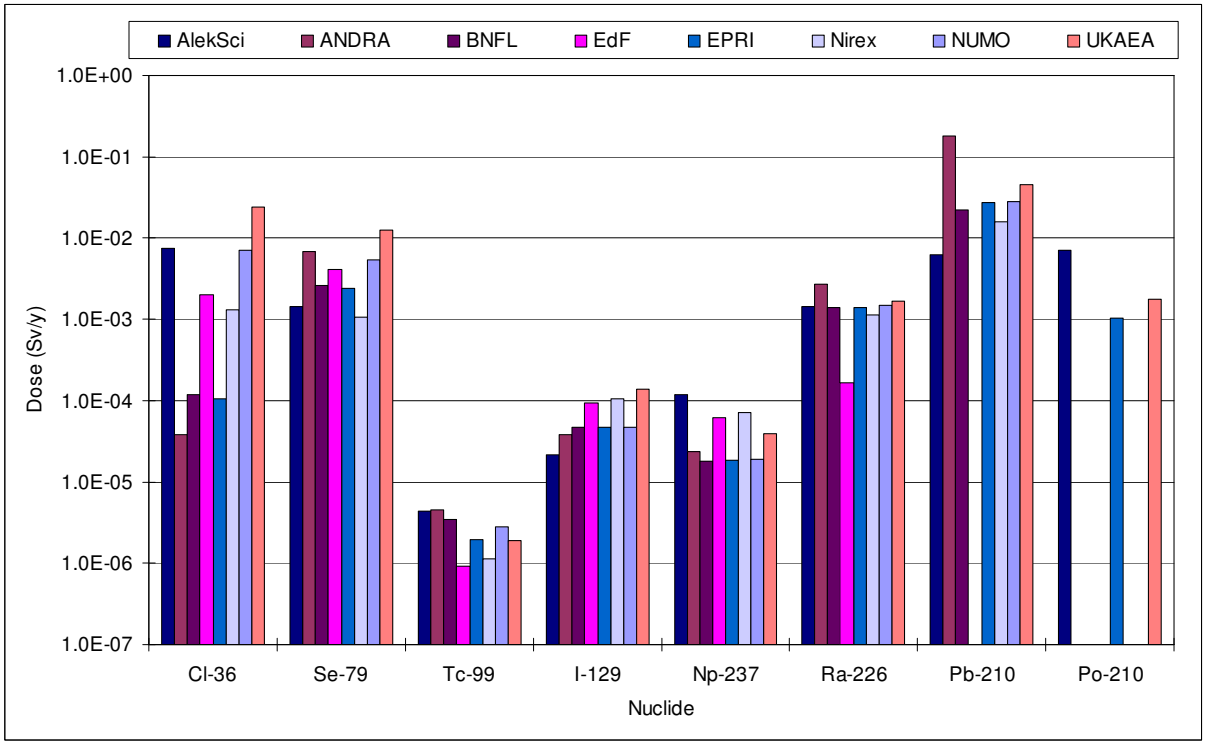


**Figure 19: Total human doses at 10,000 years**

**Table 15: Total human doses at 10,000 years [Sv/y]**

| | Cl-36 | Se-79 | Tc-99 | I-129 | Np-237 | Ra-226 | Pb-210 | Po-210 |
|---|---|---|---|---|---|---|---|---|
| AlekSci | 7.4E-03 | 1.4E-03 | 4.4E-06 | 2.2E-05 | 1.2E-04 | 1.4E-03 | 6.4E-03 | 7.1E-03 |
| ANDRA | 3.8E-05 | 6.8E-03 | 4.5E-06 | 3.8E-05 | 2.4E-05 | 2.7E-03 | 1.8E-01 | |
| BNFL | 1.2E-04 | 2.6E-03 | 3.4E-06 | 4.7E-05 | 1.8E-05 | 1.4E-03 | 2.2E-02 | |
| EDF | 2.0E-03 | 4.1E-03 | 9.1E-07 | 9.3E-05 | 6.2E-05 | 1.6E-04 | | |
| EPRI | 1.1E-04 | 2.4E-03 | 1.9E-06 | 4.7E-05 | 1.8E-05 | 1.4E-03 | 2.7E-02 | 1.0E-03 |
| Nirex | 1.3E-03 | 1.1E-03 | 1.1E-06 | 1.1E-04 | 7.1E-05 | 1.1E-03 | 1.6E-02 | |
| NUMO | 7.1E-03 | 5.4E-03 | 2.8E-06 | 4.7E-05 | 1.9E-05 | 1.5E-03 | 2.8E-02 | |
| UKAEA | 2.4E-02 | 1.2E-02 | 1.9E-06 | 1.4E-04 | 3.9E-05 | 1.7E-03 | 4.5E-02 | 1.8E-03 |

Differences in soil activities observed for most radionuclides will have a direct impact on the calculated dose. To compare dose rate values, results are normalised by dividing them by the associated soil activity (Figure 20). There is generally good agreement, except for Cl-36 modelled by ANDRA; Se-79 modelled by EDF; I-129 modelled by EDF and Nirex; Np-237 modelled by AlekSci, EDF and Nirex; Ra-226 modelled by AlekSci and EDF and Pb-210 modelled by ANDRA. The good agreement reflects on the similarity of modelling approaches used to calculate the dose rate.

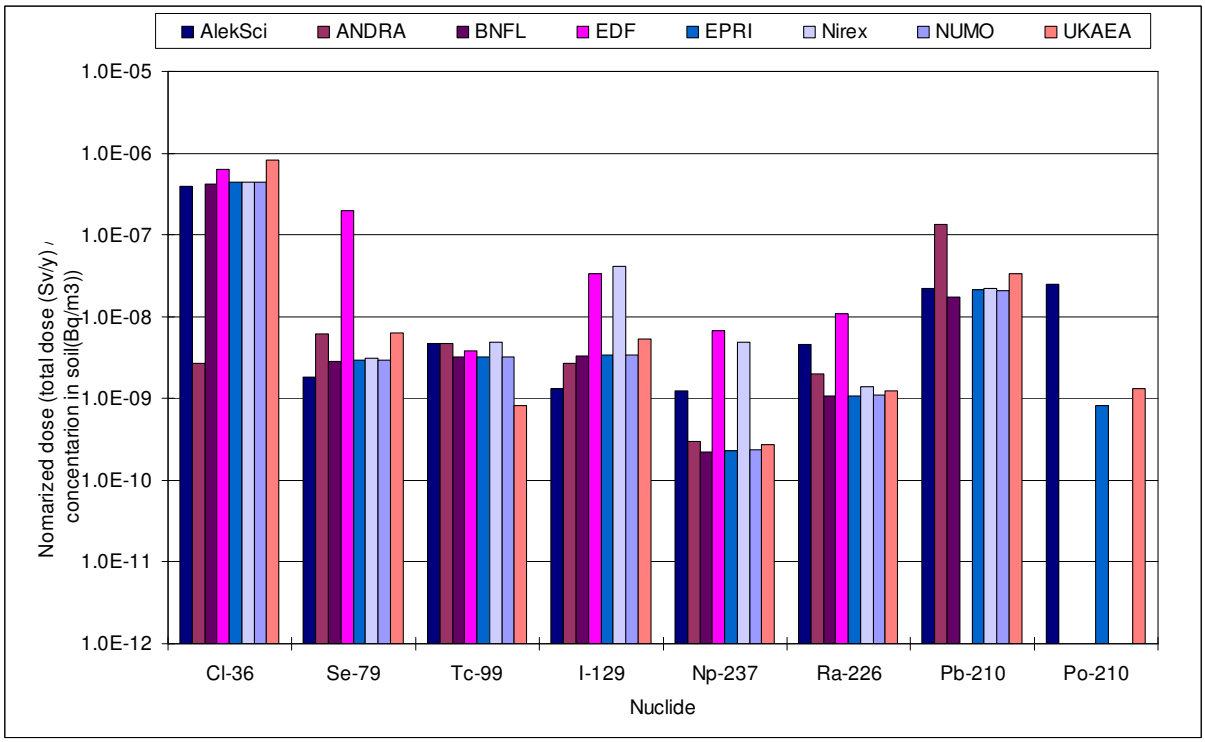


**Figure 20: Modelled total dose rate for different radionuclides as a consequences of accumulation in the soil for a period of 10,000 years, normalised to the soil radionuclide activity**

The contribution of each individual exposure pathway to the total dose is shown in Figure 21 for Cl-36, Se-79, Tc-99 and I-129 and in Figure 22 for Np-237, Ra-226 and its daughters. The contribution of each exposure pathways for Cl-36 does not dramatically vary between the individual participants. The exceptionally large contribution of milk to the total dose of Cl-36, modelled by ANDRA should be verified also in view of the overall lower total dose obtained for Cl-36 by ANDRA. For dose assessment calculations for Cl-36, ANDRA now uses a specific activity approach [Albrecht, 2004; Sheppard, 2001]. The compartmental approach used for this intercomparison is no longer applied.

The followings additional points about the human dose assessment are of interest:

(A) Common points

- For Cl-36 the contribution of animal products dominates the total dose, mainly because of the exceptionally high plant uptake factor and high transfer factor for meat and milk.
- For Se-79, the large transfer factor to cow meat and liver explains the dominant contribution of these pathways.
- For Tc-99 the contribution of agricultural products dominates the total dose, mainly because of the high plant uptake factor.
- For I-129, the large transfer factor to milk explains the contribution of this pathway.

- For Np-237, drinking water, if it's modelled, dominates the exposure, if not contribution of agricultural products dominates the total dose.

- For Ra-226, the large external dose factor explains the dominant contribution of this pathway.

- For Pb-210, the contribution of milk and liver dominates the total dose, mainly because of the high transfer factor to these animal products.

- For Po-210, the large transfer factor to animal products explains the dominant contribution of these pathways.

(B) Differences

- The contribution of the soil ingestion pathway for I-129, Np-237 and Ra-226 (and its daughters) is more important in the results modelled by AlekSci compared to results supplied by others.

- EDF modelled a significantly large contribution of the meat pathway for Se-79 compared to others. The contribution of the milk pathway for Ra-226 as modelled by ANDRA is higher than the contribution modelled by others.

- EDF and Nirex considered the drinking water pathway, which was not suggested in the scenario specification. This pathway becomes significant for Tc-99, I-129 and Np-237 (EDF and Nirex, Figure 21 and Figure 22) and for Ra-226 (EDF, Figure 22). The contribution of the drinking water pathway is not significant for Cl-36 for which the contribution of agricultural products dominates the total dose because of the exceptionally high plant uptake factor. For Se-79, the large transfer factor to cow meat and liver explains the dominant contribution of these pathways. Note that Pb-210 and Po-210 are not present at the source. These are therefore initially absent in the irrigation or drinking water.

- Because of the influence of the above mentioned contributions of the drinking water pathway (Figure 21 and Figure 22), normalised doses to the radionuclide concentration in the soil of EDF and Nirex are significantly higher for I-129, Np-237 and Ra-226 for EDF, and I-129 and Np-237 for Nirex, respectively. On the other hand there is no specific difference between EDF and Nirex and the other participants in the normalised dose of Tc-99 despite the contribution of the drinking water pathway. This can be discussed in the future with detailed information about exposure modelling. The reason why the contribution of the drinking pathway of Ra-226 is much higher in the EDF calculation compared to that of Nirex, is not certain at this stage.

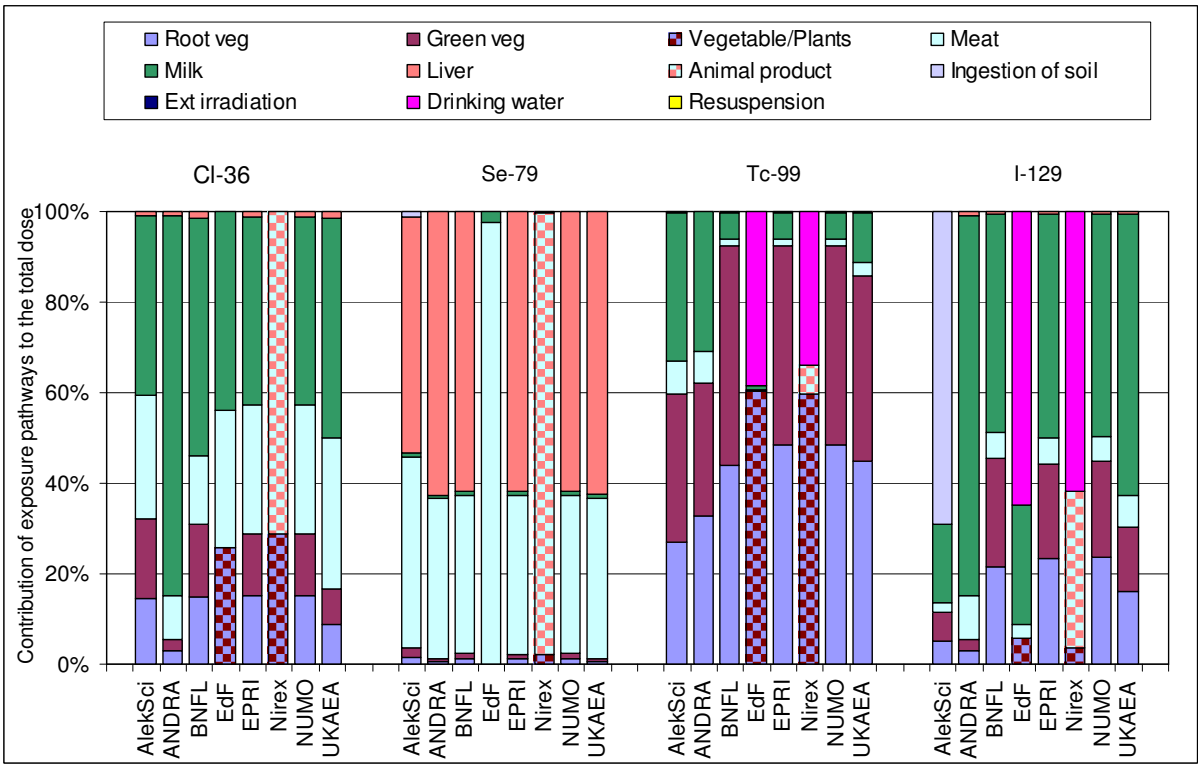


**Figure 21: Contribution of exposure pathways to the total dose at 10,000 years (Cl-36, Se-79, Tc-99 and I-129)**

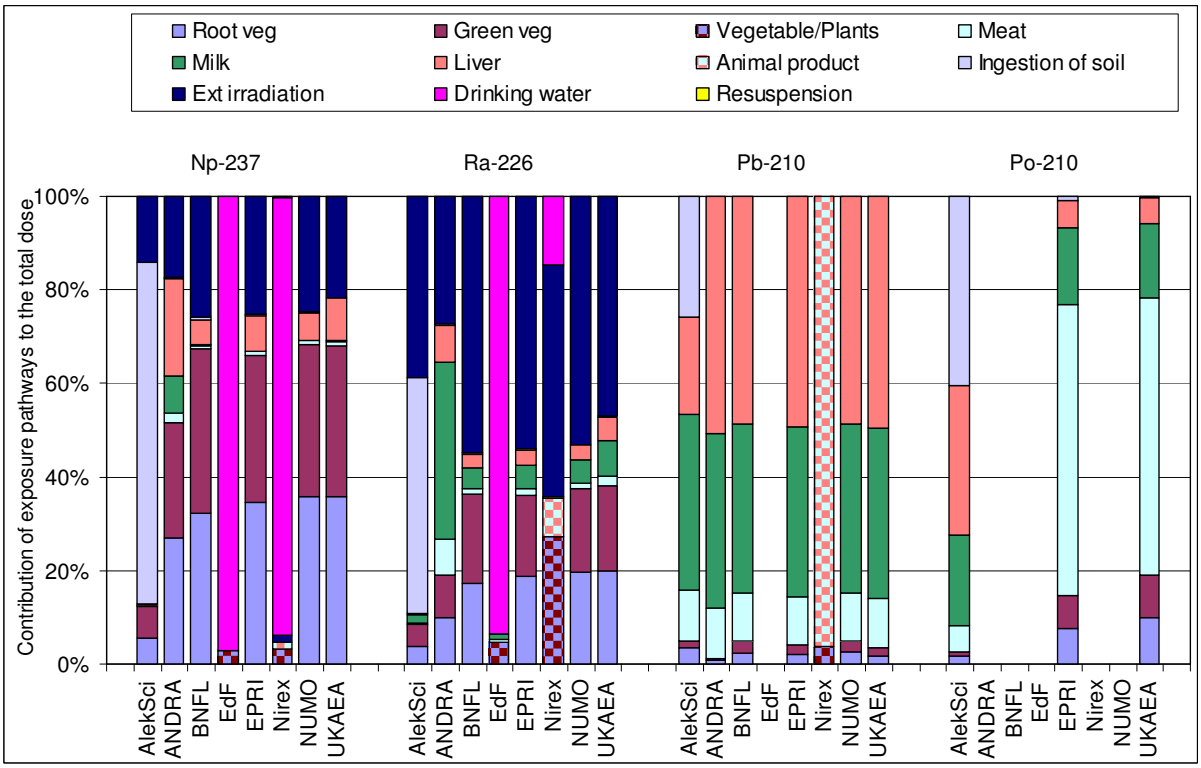


**Figure 22: Contribution of exposure pathways to the total dose at 10,000 years (Np-237, Ra-226, Pb-210 and Po-210)**

# 4. RESULTS OF THE RIVER SCENARIOS

## 4.1 Concept and approaches for the river scenario

As described in §1.2.1 the river scenario deals with the accumulation of specified radionuclides in the soil as the consequence of flooding river water (Figure 23). The goal of the intercomparison was to evaluate the different model approaches for river transport, flooding of agricultural land and the related accumulation in the soil. ANDRA, BNFL and NUMO participated in this intercomparison. It was assumed that the model approaches for dose calculations for soil contaminated by irrigation and inundation are identical. It was therefore decided to carry out intercomparison calculations only on the soil compartment. This avoided unnecessary duplication between the river and well scenarios.

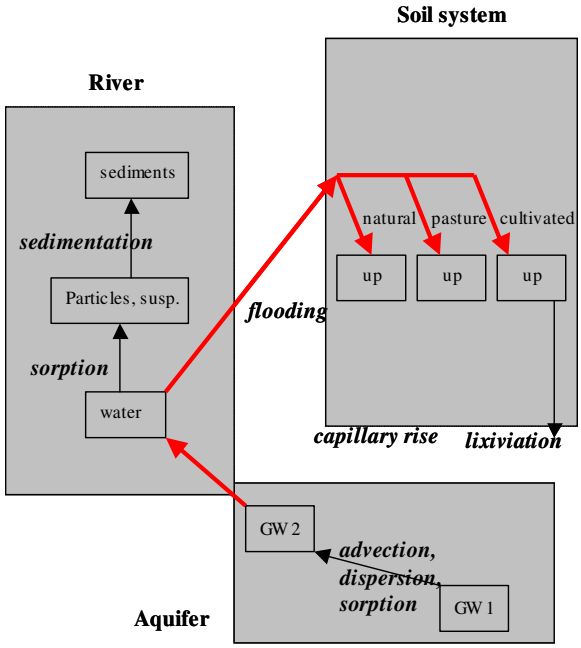


**Figure 23 : Schematic representation of flooding river water contaminating agricultural soil**

For the river scenario, all three participants set flooding rate and leaching rate as 5.5E-04 m/y and 5.5E-02 m/y respectively. ANDRA and NUMO used the same models for the calculations of the river and well scenarios. BNFL used a different approach, integrating the mathematical equations that describes the single compartment soil model within an Excel spread sheet.

## 4.2 Results

The activities of radionuclides in the soil compartment calculated by the three participants are given as a function of time (Figure 24). The results at 10,000 years (equilibrium concentration) are also summarised in Table 16. There are no meaningful discrepancies between the three participants except for Tc-99, for which the result of BNFL at 10,000 years is 1.46 times higher than the result obtained by NUMO.

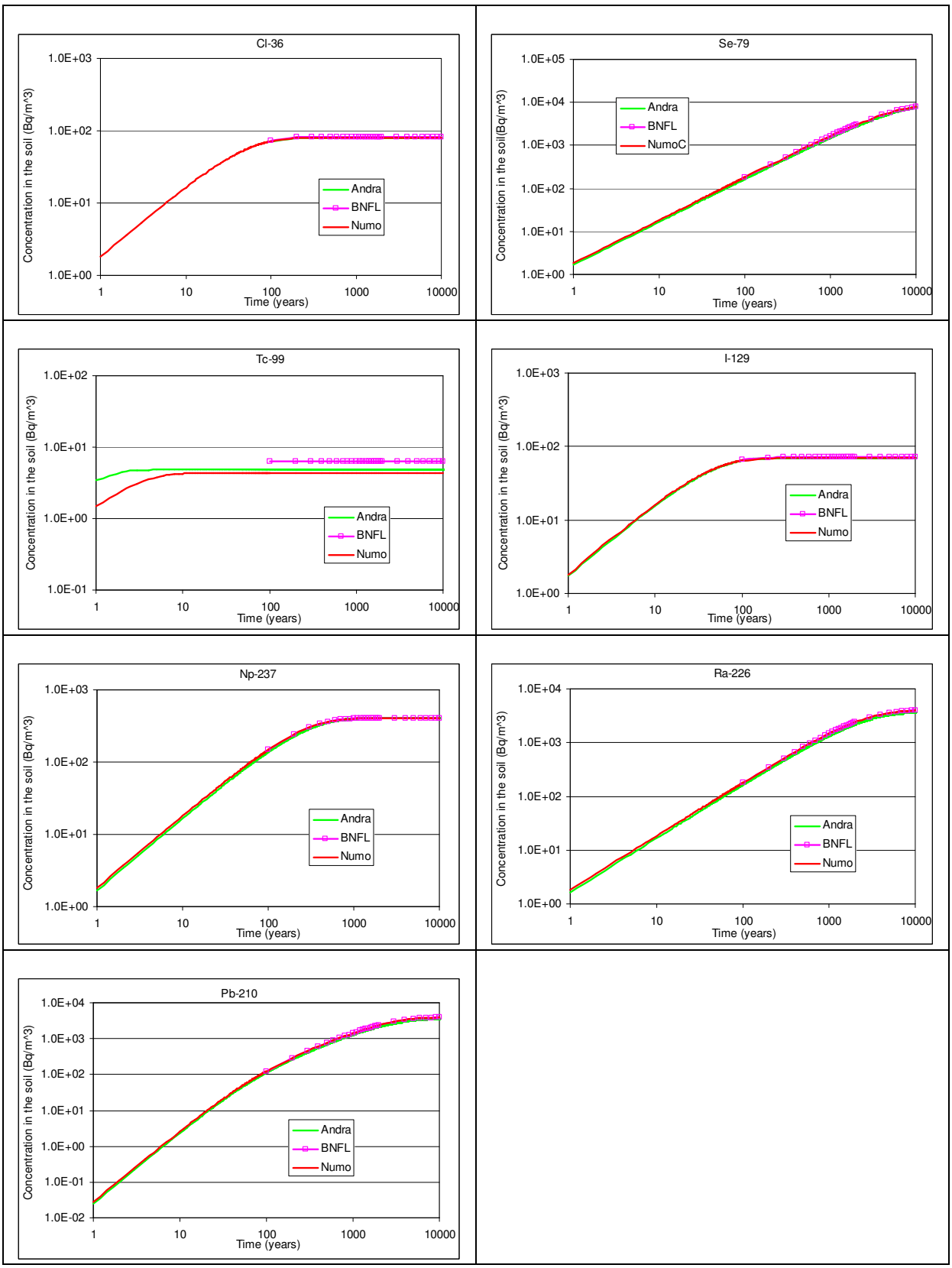


**Figure 24: Radionuclide concentration in the soil for river scenario [Bq/m$^3$] as a function of time as modelled by the different participants (log-log scale)**

**Table 16: Radionuclide concentration in the soil at 10,000 years river scenario [Bq/m$^3$]**

| | Cl-36 | Se-79 | Tc-99 | I-129 | Np-237 | Ra-226 | Pb-210 |
|---|---|---|---|---|---|---|---|
| ANDRA | 8.0E+01 | 7.7E+03 | 4.8E+00 | 7.0E+01 | 4.0E+02 | 3.6E+03 | 3.6E+03 |
| BNFL | 8.2E+01 | 8.0E+03 | 6.3E+00 | 7.1E+01 | 4.0E+02 | 4.0E+03 | 3.9E+03 |
| NUMO | 8.0E+01 | 8.0E+03 | 4.3E+00 | 6.9E+01 | 4.0E+02 | 3.9E+03 | 3.9E+03 |

As seen from Table 16 and the related figures, soil activities modelled by the 3 participants are either identical or insignificantly different. Mathematical approaches are comparable amongst the 3 groups and identical in comparison with the well scenario calculations. The similarity between results from the three groups is larger than that observed during the well scenario. This is mostly related to the fact that BNFL did not consider cropping loss, as was done during the earlier exercise.

## 4.3 Discussion

The results of river scenario can be analysed by checking the loss rates from soil compartment as was done for the well scenario. Loss rates calculated by BNFL and NUMO modelling are summarized in Table 17. The total loss rate, which is defined by the sum of radioactive decay and percolation/leaching loss, is mostly identical for all radionuclides except for Tc-99 (see also difference of Tc-99 soil concentration; Figure 24). The difference of percolation/leaching loss arises from the slightly different mathematical expressions between BNFL and NUMO (§3.1.2). This difference is negligible as sorption coefficients become larger.

**Table 17: Summary of loss rates calculated by BNFL and NUNO modelling for river scenario**

| | Decay [1/y] | Percolation or leaching loss [1/y] | | total loss [1/y] | |
|---|---|---|---|---|---|
| | BNFL / NUMO | BNFL | NUMO | BNFL | NUMO |
| Cl-36 | 2.30E-06 | 2.24E-02 | 2.30E-02 | 2.24E-02 | 2.30E-02 |
| Se-79 | 1.10E-05 | 1.87E-04 | 1.87E-04 | 1.98E-04 | 1.98E-04 |
| Tc-99 | 3.30E-06 | 2.90E-01 | 4.24E-01 | 2.90E-01 | 4.24E-01 |
| I-129 | 4.40E-08 | 2.57E-02 | 2.65E-02 | 2.57E-02 | 2.65E-02 |
| Np-237 | 3.20E-07 | 4.55E-03 | 4.58E-03 | 4.56E-03 | 4.58E-03 |
| Ra-226 | 4.30E-04 | 2.77E-05 | 2.77E-05 | 4.58E-04 | 4.58E-04 |
| Pb-210 | 3.10E-02 | 2.56E-04 | 2.56E-04 | 3.13E-02 | 3.13E-02 |

The ratios of equilibrium concentrations between the river and the well scenarios are shown in Figure 25. Theoretically, this ratio should be 0.005 as conceptual and mathematical modelling approaches are identical and the only difference between the river and well scenarios is the contamination rate (irrigation or flooding).

From Figure 25, the following points can be derived.

- Except for the BNFL results for Cl-36, Se-79 and Tc-99, the ratio between the river and well scenarios are comparable to 0.005. This indicates that infiltration losses dominate the radionuclide concentrations in the soil.

- Result from BNFL are different from 0.005 for Cl-36, Se-79, Tc-99, Ra-226 and Pb-210. This is related to the consideration of cropping which is modelled by BNFL only for the well scenario.

- For Ra-226 and Pb-210, all three participants get a smaller ratio than 0.005. This indicates that radioactive decay can not be ignored in comparison with percolation/leaching loss for those radionuclides.

.

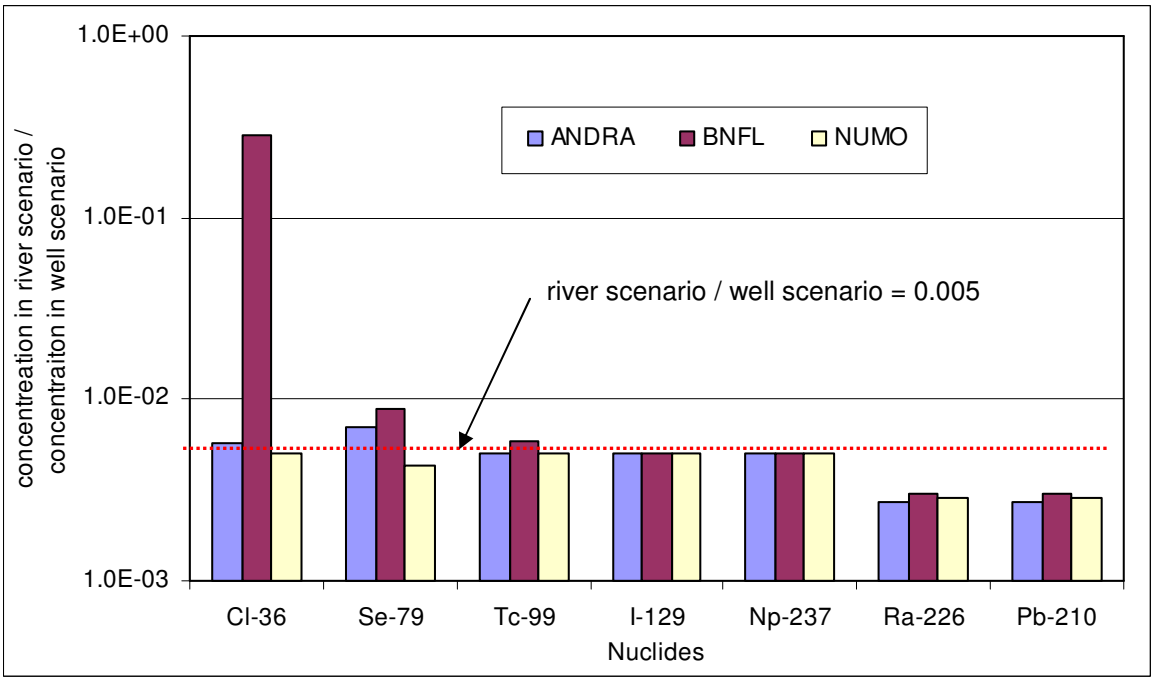


**Figure 25: Comparison of concentration in the soil between well scenario and river scenario**

# 5. SUMMARY AND CONCLUSIONS

**Well scenario**

Radionuclide concentration

- For the well scenario, 8 organisations participated and calculated radionuclide concentrations in soil with reasonable agreement, and explainable exceptions.
- Cropping processes were modelled by some, but not by others. This decreased the radionuclide concentration in the soil for those radionuclides with high soil to plant transfer coefficient such as Cl-36, Se-79 and Tc-99.
- Slightly different modelling approaches for percolation loss were applied. Their impact was largest for low Kd radionuclides such as Tc-99.
- Lower irrigation rates as depicted by some participants reduces soil concentrations and related overall doses.
- Modelling of seasonal change generally reduces soil concentrations. Differences between summer and winter is most significant for Tc-99 (more than a factor of 2).
- Consideration of a lower soil compartment can either reduce the upper soil compartment concentration (Radionuclide mixed into a larger soil section) or increase it by transferring radionuclide back via capillary rise.

**Exposure dose**

- Difference of the calculated total doses are, in most cases, explained by difference in the associated soil concentration.
- Consideration of the drinking water pathway (as was done by some participants) increased the total dose in particular for Tc-99, I-129, Np-237 and Ra-226.

**River Scenario**

- Three organisations participated in calculation for a river scenario. They obtained compatible results except for the low Kd radionuclide Tc-99 for which differences in percolation modelling becomes apparent.
- The ratio of radionuclide concentrations in the soil between the well and river scenarios shows good agreement to the analytically estimated value of 0.005.

## 6. REFERENCES

Albrecht, A. (2004). Intégration dans le code de calcul Aquabios d'un modèle du comportement de Cl-36 dans la biosphère basée sur le rapport isotopique et analyse de sensibilité, Note Technique *C NT ASTR 04-007*, 34 pp., ANDRA, Châtenay-Malabry.

Albrecht, A. & Bonafos, C. Aquabios, (2004). A programme for the implementation of biosphere contaminant transfer assessment models, linkage to databases and reporting tools. BROWNFIELDS 2004, Siena.

ANDRA (2003). AQUABIOS database, 2003.

BIOPROTA (2003). First year progress report, version 1.0, draft, November 2003.

Ciffroy P., Siclet F., Damois C. (to be published). A dynamic model for assessing radiological consequences of routine releases in rivers - Part1: description of the model and parameter values.

Coughtrey P J, Jackson D, Thorne M C. (1983-85). Radionuclide Distribution and Transport in Terrestrial and Aquatic Ecosystems. Volumes 1-6. AA Balkema, Rotterdam.

EPRI (2002). Evaluation of the Proposed High Level Radioactive Waste Repository at Yucca Mountain Using Total System Performance Assessment, Phase 6, Technical Report 1003031.

IAEA (2003). "Reference Biospheres" for solid radioactive waste disposal, Note Technique *IAEA_BIOMASS-6*, 560 pp., Internatioanl Atomic Energy Agency, Vienna.

ICRP (1996). ICRP Publication 72, Age dependent Doses to members of the Public from Intake of Radionuclides: Part 5. International Commission on Radiological Protection, Pergamon Press.

JNC (2000). H12: Project to establish the Scientific and Technological Basis for HLW Disposal in Japan – Safety Assessment of the Geological Disposal System, JNC TN1410 2000-004, Tokai-Mura.

Klos, R. (2000). A Mathematical Description of Components and Processes in Compartmental Representations of the Physical Environment, Note Technique *ASAN 00-01*, 12 pp., Aleksandria Sciences, Sheffield.

Klos, R. A., H. Müller-Lemans, F. van Dorp, and P. Gribi (1996). TAME - The Terrestrial-Aquatic Model of the Environment: Model definition, Note Technique *93-04*, 173 pp., NAGRA, Wettingen, Switzerland.

Klos, R. A., I. Simón, U. Bergström, A. M. Uijt de Haag, C. Valentin-Ranc, T. Zeevaert, J. A. K. Reid, P. Santucci, J. Titley, and J. Stansby (1999). Complementary studies: biosphere modelling for dose assessments of radioactive waste repositories, *J. Environ. Radioactivity*, 42, 237-254.

Sheppard, M. (2001). Transfer of Chlorine 36 in the biosphere: bibliography and modelling, Note Technique *C RP 0ECO 2000/04/A*, 114 pp., ANDRA, Châtenay-Malabry.

Thorne, M C (2003a). Derivation of Biosphere Factors for use in the Drigg Post-Closure Radiological Safety Assessment, Mike Thorne and Associates Limited Report MTA/P0012/2002-1: Issue 2.

Thorne, M C (2003b). A Guide to the Spreadsheet Calculations for the Generic Performance Assessment, Mike Thorne and Associates Limited Report MTA/P0011D/2002-2; Issue 2.

Walke, R.C., Longworth, J.K., Little, R.H. & Smith, G.M (2004). The Practical Application of the AMBER Software Tool to Support Environmental Decision Making. BROWNFIELDS 2004, Siena.

Willans S.M. (2003). Program User's Guide for the MONDRIAN Biosphere Code, BIOS Version 4.3. BNFL R&T report EN0055/8/25 Issue 2.

# 1. APPENDIX A: ANALYTICAL SOLUTION OF THE EQUATION GOVERNING THE RADIONUCLIDE ACTIVITY IN THE SOIL: APPROXIMATE EXPRESSION

## 1. Analytical Solution

The general mathematical expression of activity of radionuclide *N* in the soil compartment is:

$$\frac{dN}{dt} = S(t) - \lambda_N N - \lambda_{CH} N - \lambda_I N \quad (1)$$

where,

| | |
|---|---|
| *N* | is the activity of radionuclide *N* in the soil compartment, (Bq) |
| *S(t)* | is an external source term of radionuclide *N* to soil compartment (flooding), (Bq/y) |
| $\lambda_N$ | is the decay constant for radionuclide *N*, (1/y) |
| $\lambda_{CH}$ | is the loss rate by the cropping for radionuclide *N*, (1/y) |
| $\lambda_I$ | is the loss rate by the infiltration for radionuclide *N*, (1/y) |

This equation can be solved with an initial activity of zero and a constant source term as follows.

**Cl-36, Sr-79, Tc-99, I-129, Np-237 and Ra-226**

$$N(t) = \frac{S}{\lambda}\left[1 - \exp(-\lambda t)\right] \quad (2)$$

where,

$$\lambda = \lambda_N + \lambda_I + \lambda_{CH} \quad \text{or} \quad \lambda = \lambda_N + \lambda_I \quad \text{if} \quad \lambda_{CH} = 0$$

**Treatment of a decay chain (i.e. Pb-210)**

Pb-210 is a decay product of Ra-226. The source term of Pb-210 ( $S^{Pb\text{-}210}(t)$ ) is given by:

$$S^{Pb210}(t) = \lambda_N{}^{Ra226} N^{Ra226}(t) = \lambda_N{}^{Ra226} \cdot \frac{S^{Ra226}}{\lambda^{Ra226}}\left[1 - \exp\left(-\lambda^{Ra226} t\right)\right] \quad (3)$$

where,

| | |
|---|---|
| $\lambda_N{}^{Ra226}$ | is the decay constant of Ra-226, (1/y) |
| $N^{Ra226}$ | is the activity of Ra-226 in the soil compartment, (Bq) |
| $\lambda^{Ra226}$ | is the total loss rate of Ra-226, defined by $\lambda^{Ra226} = \lambda^{Ra226}{}_N + \lambda^{Ra226}{}_I$, (1/y) |
| $S^{Ra226}$ | is an external source term of Ra-226 to soil compartment (flooding), (Bq/y) |

Then, the rate at which the activities of Pb-210 changes with time is given by,

$$\frac{dN^{Pb210}}{dt} = \frac{\lambda_N^{Ra226} S^{Ra226}}{\lambda^{Ra226}}\left[1-\exp\left(-\lambda^{Ra226}t\right)\right]-\lambda^{Pb210}N^{Pb210}$$

This can be solved as follows with an initial activity of zero for both of Ra-226 and Pb-210, and a constant source term of Ra-226

$$N^{Pb210} = \frac{\lambda_N^{Ra226} S^{Ra226}}{\lambda^{Ra226}}\left\{\frac{1}{\lambda^{Pb210}}\left[1-\exp\left(-\lambda^{Pb210}t\right)\right]-\frac{1}{\lambda^{Pb210}-\lambda^{Ra226}}\left[\exp\left(-\lambda^{Ra226}t\right)-\exp\left(-\lambda^{Pb210}t\right)\right]\right\}$$

(4)

## 2. Approximate Expression

Equation (2) can be expressed using a Taylor expansion as follow.

$$N(t) = \sum_{n=1}^{\infty}\frac{(-t)^n}{n!}N^{(n)}(t)$$

$$= N(0)-t\cdot\left.\frac{dN(x)}{dx}\right|_{x=0}+\frac{t^2}{2}\left.\frac{d^2N(x)}{dx^2}\right|_{x=0}-\frac{t^3}{6}\left.\frac{d^3N(x)}{dx^3}\right|_{x=0}+\ldots\ldots$$

And for small *t*, this Taylor expansion of *N(t)* can be simplified as a approximation of the original equation (2)

$$N(t) \cong N(0)-t\cdot\left.\frac{dN(x)}{dx}\right|_{x=0}$$

$$= \frac{S}{\lambda}\{1-\exp(0)\}-t\cdot\left[(-\lambda)\frac{S}{\lambda}\{1-\exp(x)\}\right]_{x=0}$$

$$= St$$

On the other hand equation (2) is apparently close to $S/\lambda$ as $t\rightarrow\infty$.

# 2. APPENDIX B: RADIONUCLIDE CONCENTRATIONS WITH THE CONDITION OF INCREASED IRRIGATION RATE IN EDF MODELLING FACTOR OF 2.66

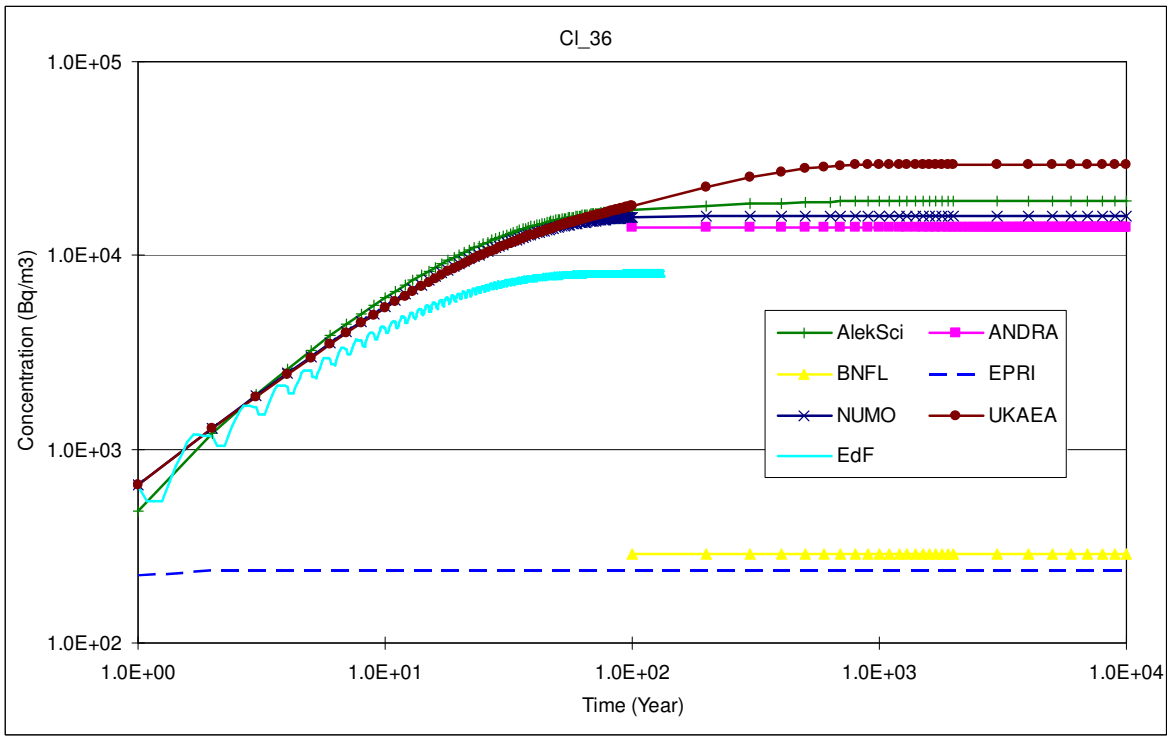


**Figure 26: Radionuclide concentration in the soil with the increased irrigation rate of EDF (Cl-36)**

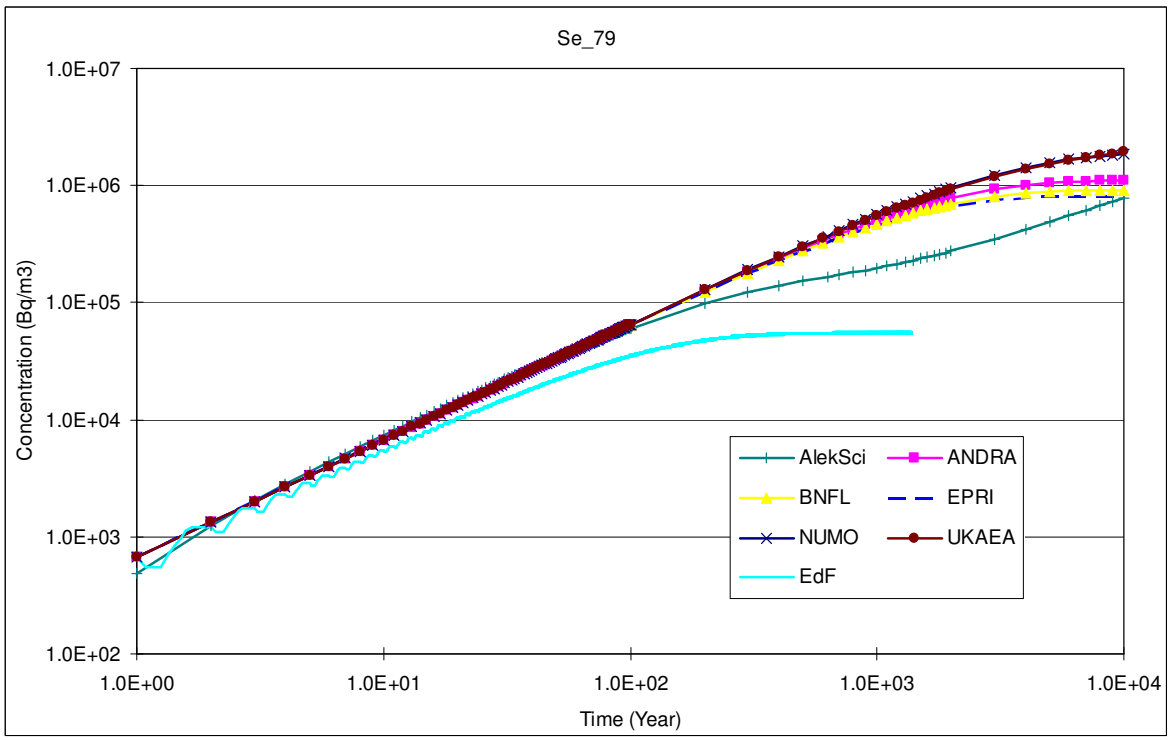


**Figure 27: Radionuclide concentration in the soil with the increased irrigation rate of Ed (Se-79)**

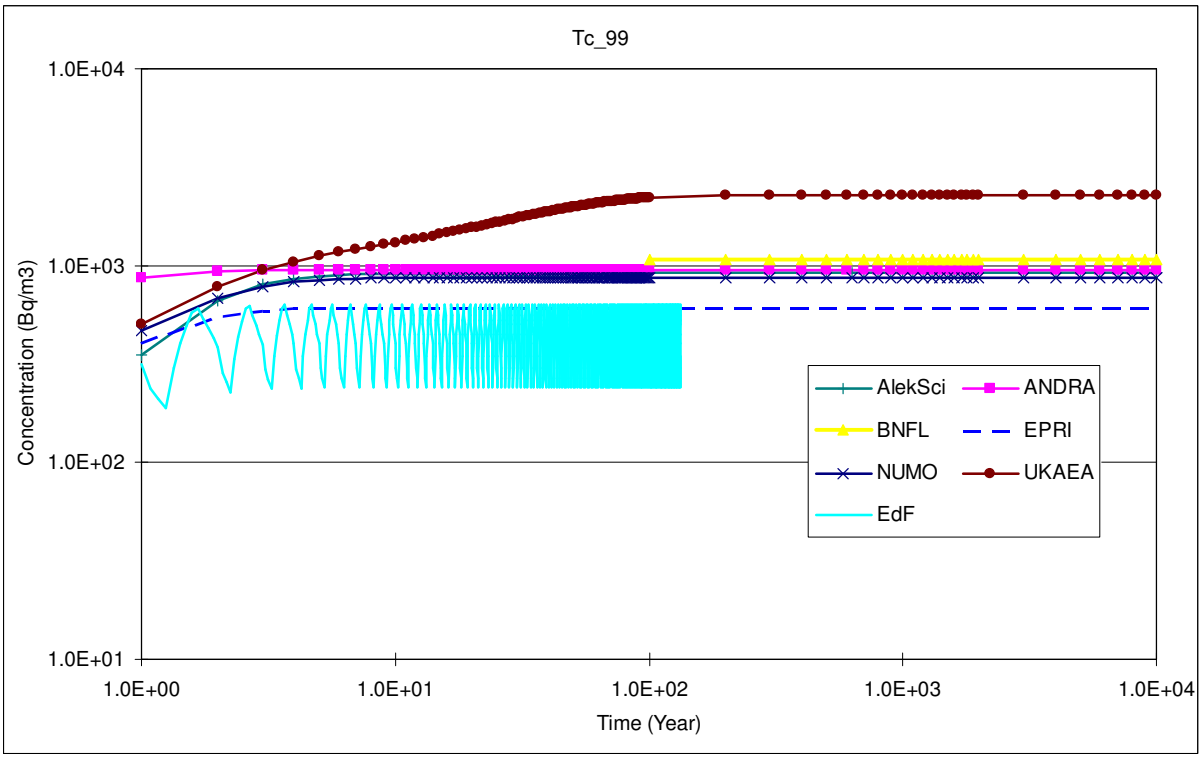


**Figure 28: Radionuclide concentration in the soil with the increased irrigation rate of EDF (Tc-99)**

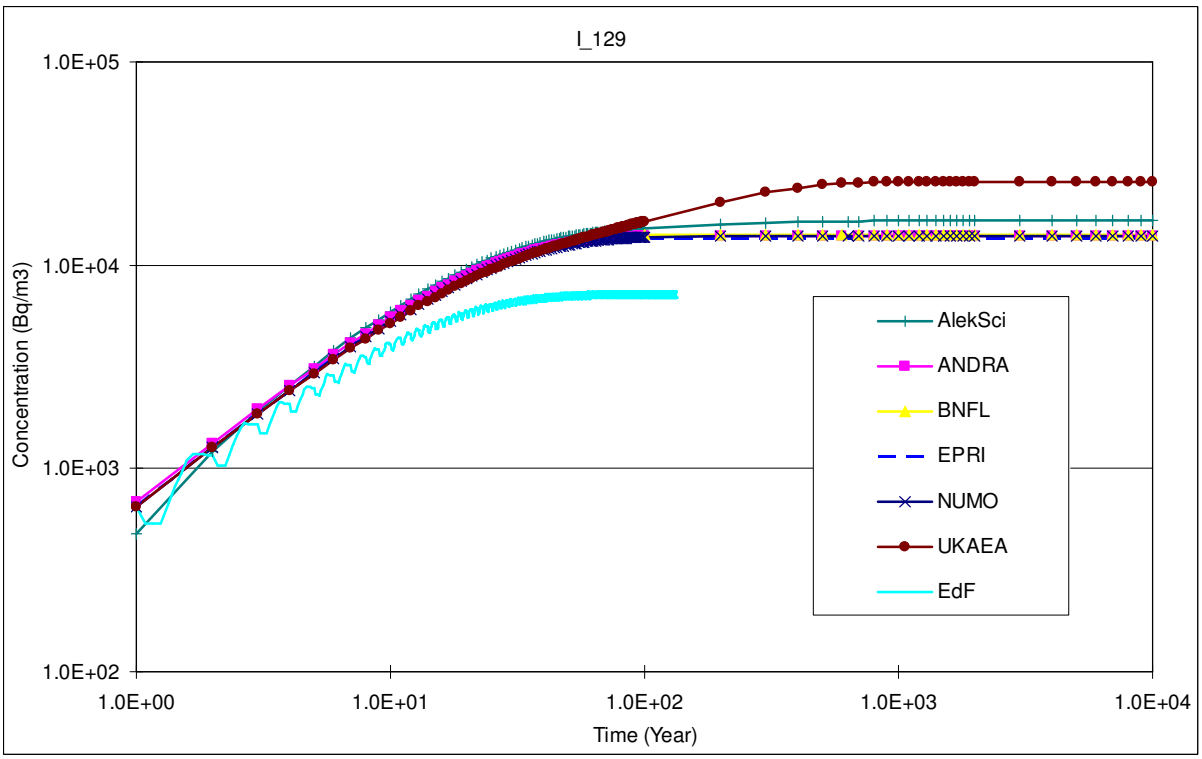


**Figure 29 Radionuclide concentration in the soil with the increased irrigation rate of EDF (I-129)**

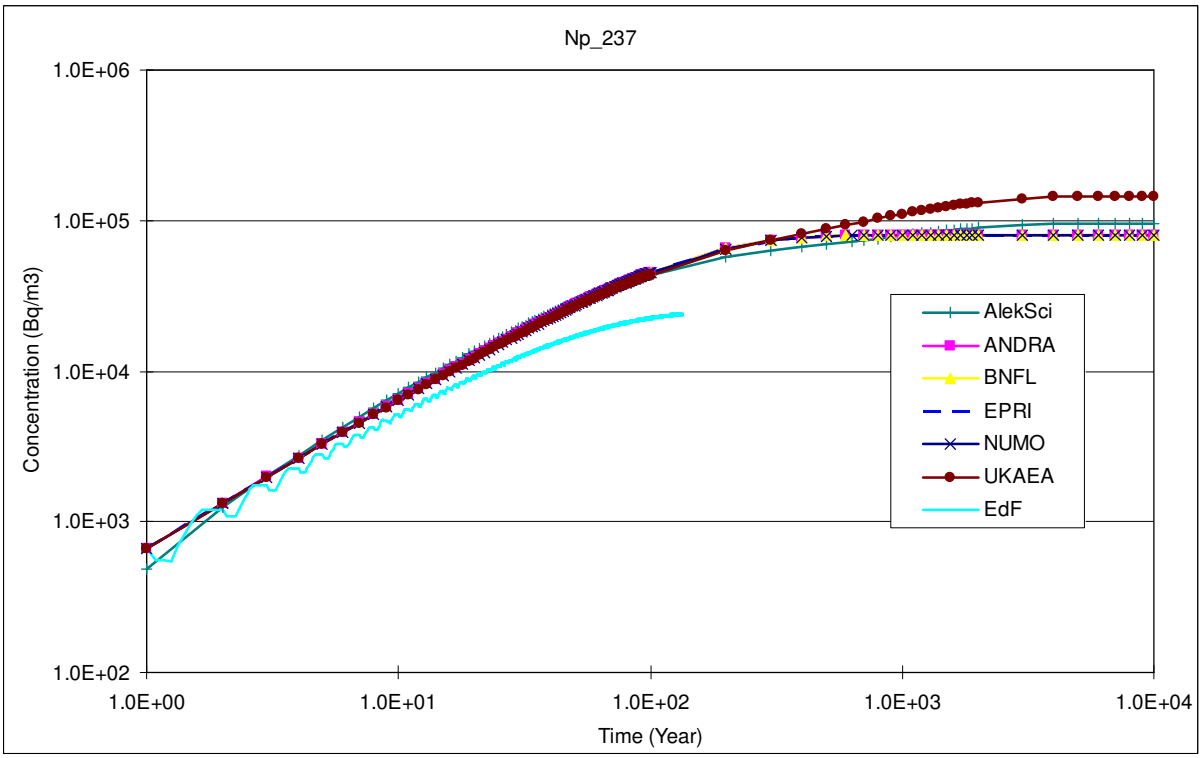


**Figure 30: Radionuclide concentration in the soil with the increased irrigation rate of EDF (Np-237)**

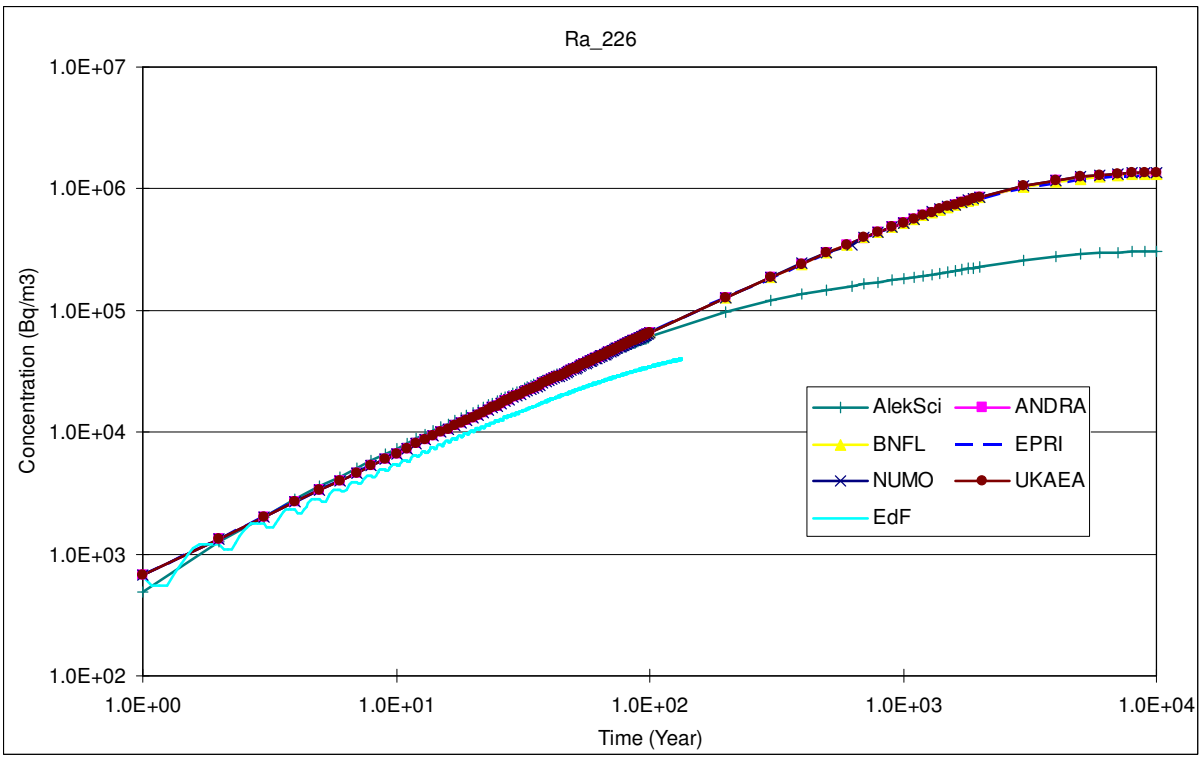


**Figure 31 Radionuclide concentration in the soil with the increased irrigation rate of EDF (Ra-226)**

# 3. APPENDIX C: RADIONUCLIDE CONCENTRATIONS IN THE SOIL, SATURATED ROCK AND UNSATURATED IN UKAEA MODELLING

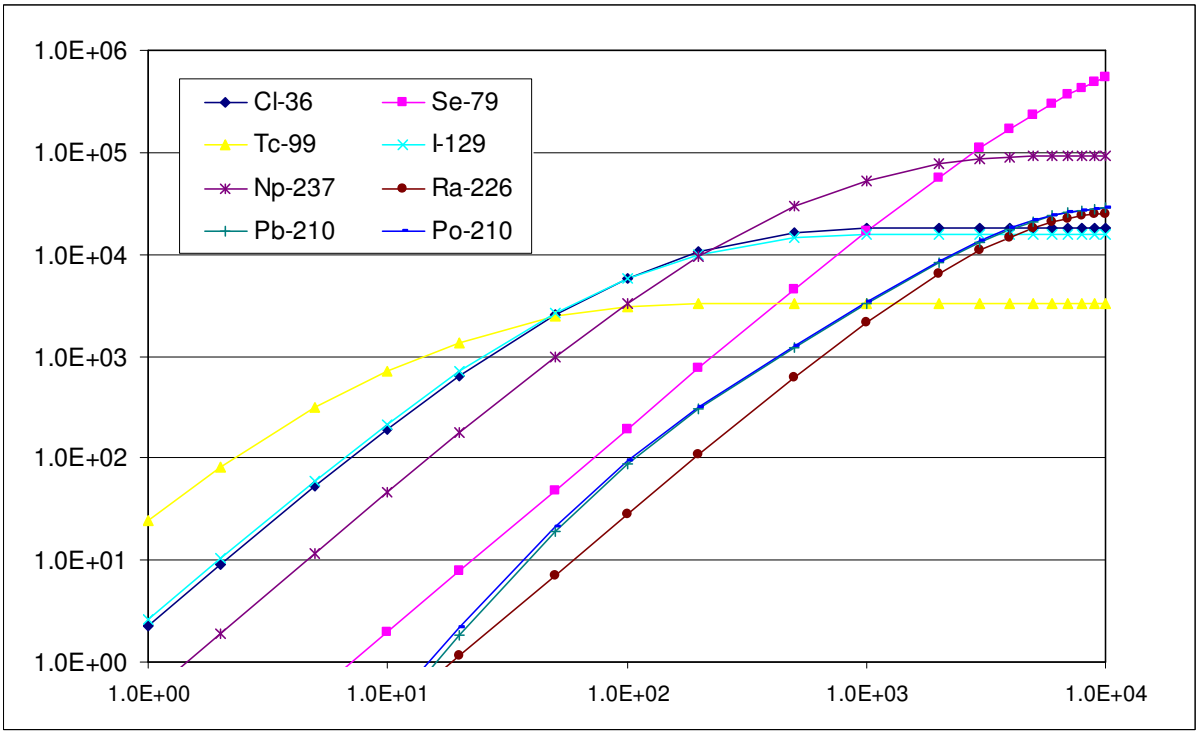


**Figure 32: Radionuclide concentration in the soil in UKAEA modelling**

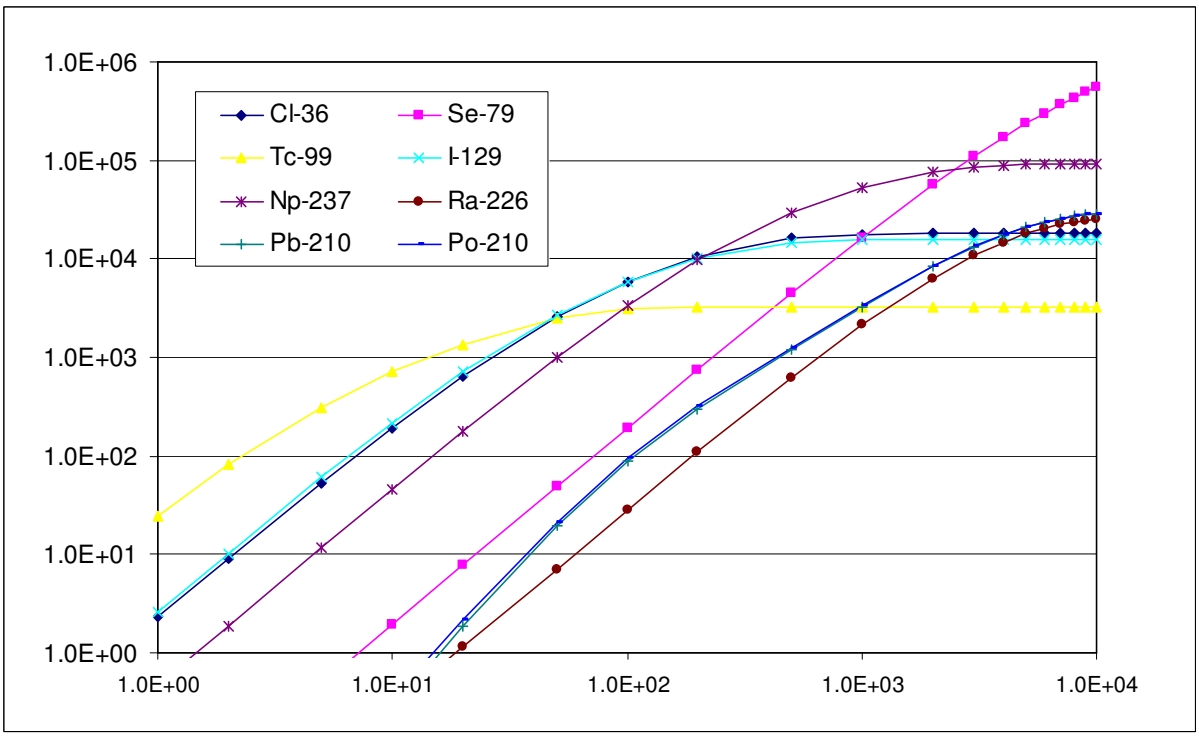


**Figure 33: Radionuclide concentration in the unsaturated rock in UKAEA modelling**

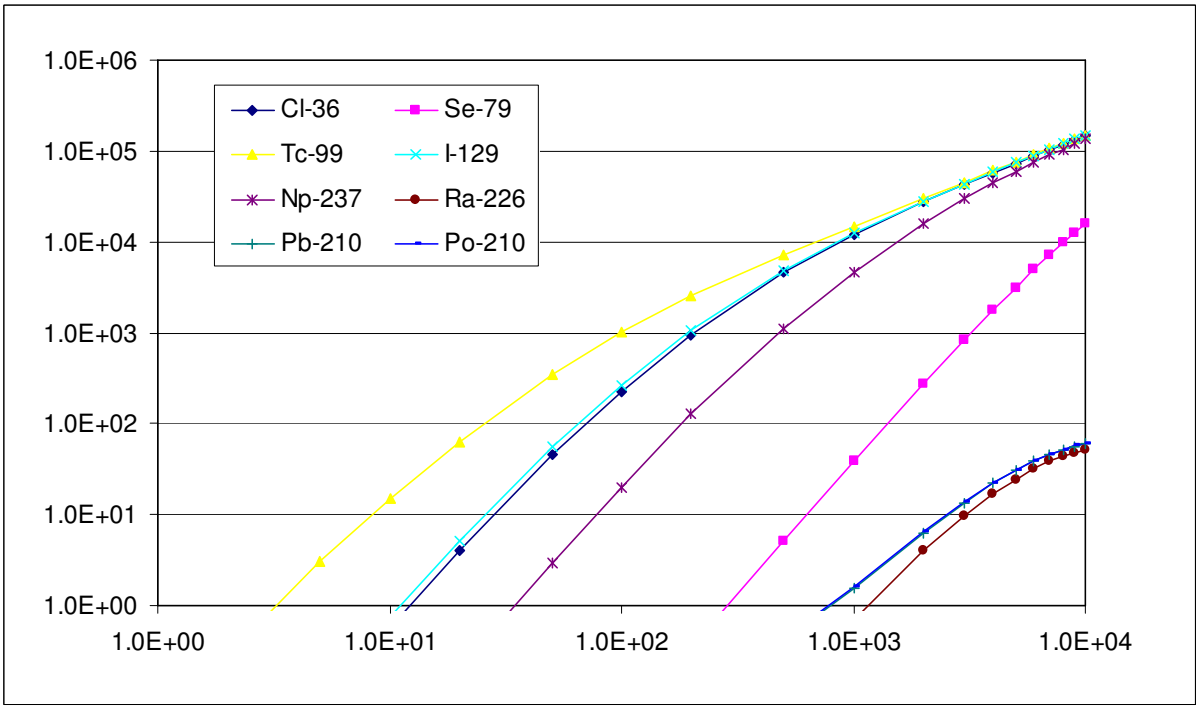


**Figure 34: Radionuclide concentration in the saturated rock in UKAEA modelling**